The Pennsylvania State University

The Graduate School

Department of Aerospace Engineering

CONTROLLABLE ELASTIC COUPLING OF COMPOSITE MULTI-LAYER BEAMS

A Thesis in

Aerospace Engineering

by

Alvord Marques

Submitted in Partial Fulfillment
of the Requirements
for the Degree of

Master of Science

August 2008

The thesis of Alvord Marques was reviewed and approved* by the following:

Farhan Gandhi
Professor of Aerospace Engineering
Thesis Advisor

Timothy F. Miller
Senior Research Associate, Applied Research Lab

George A. Lesieutre
Professor of Aerospace Engineering
Head of the Department of Aerospace Engineering

*Signatures are on file in the Graduate School

ABSTRACT

This thesis presents the analysis of controllable elastic couplings of composite multi-layer beams using polymer layers in different temperature states. The multi-layered beam consists of a base layer of a two-ply composite laminate with polymer layers on the upper and lower surfaces sandwiched between two composite cover layers. The stiffness variation is based on the concept that when the polymer layer is stiff, the cover composite layers are strongly coupled to the base layers and the beam behaves as an integral unit on application of a bending or extensional load. However, if the shear modulus of the polymer layer is reduced, the cover layers are largely decoupled from the base layers and the stiffness is dominated by the base layers. The shear modulus of the polymer layer is reduced by increasing its temperature through glass transition. The analysis includes development of stiffness metrics to characterize the beam stiffness in the coupled and decoupled states on the application of a bending and extensional load respectively. Various ply orientations were analyzed to determine the laminate configuration that would produce maximum value in the stiffness metrics. The effects of the polymer layer on the coupling of the system were analyzed through ANSYS and the trend in the results was in good agreement with the theory. The metrics determined the choice of laminate ply angle layup to ensure that the extensional and torsional stiffness of the system were not adversely affected due to the coupling of the plies.

TABLE OF CONTENTS

LIST OF FIGURES

LIST OF TABLES

ACKNOWLEDGEMENTS

I want to take this opportunity to dedicate this work to my parents Felix and Muriel Marques and sister Alina without whose guidance, help, support and encouragement I would never have been able to achieve this milestone. Their unconditional love and tremendous encouragement translated into many hurdles being overcome during this important stage of my academic career. I am forever indebted to my mother for giving me the best advice that time spent is time gained and for being there with me when I needed it. I also dedicate this work to my father who has worked so hard and made so many sacrifices to give me this chance of realizing my dream.

Ever since I can remember, I have always dreamt of one day becoming an Aerospace Engineer. Words desert me in expressing my gratitude to all those who have made this dream possible. I wish to express my sincere gratitude to my advisor, Dr. Farhan Gandhi of the Penn State Aerospace Engineering department. I use this opportunity to thank him for his time, effort and most importantly his infinite patience he exercised on me during the course of my research. I also thank him for providing me with an opportunity to work under him. I am proud of his support. I also want to thank Dr Timothy Miller who has so graciously offered his time and advice in reading my thesis.

I am obliged to Dr. Ed Smith who guided me through the course of my early undergraduate career, never a hesitation in his guidance. I am also extremely thankful to Dr. Stephen Conlon and Dr. George Lesieutre for giving me an opportunity to work as a teaching assistant under their guidance which has molded me into an all-rounded individual and I also acknowledge their confidence in me in letting me take the Lead Teaching Assistant roles.

I am thankful to Gabriel Murray, Raymond Olympio, Bilim Atli, Kirsten Bossenbroek and Dr. Thomas Juska who helped me with various aspects of my research. This is also an opportunity for me to thank Richard Auhl for his unconditional support and timely help throughout the course of my academic career and training me to use laboratory facilities. I also thank the staff notably Amy, Janice, Mark, Rhonda, all the Debbies, undergraduate and graduate department heads Dr Melton and Dr Spencer

without whom I may have never been able to achieve this honor. They have never run short of things they share; advice, guidance, assistance, even a smile each day.

Many friends at Penn State who are too many to name, deserve credit for supporting me during the difficult times and for being there with me during the good time. I wish to thank all my undergraduate friends whose constant cooperation reflected in my performance. Special thanks to Diana Valtierra, Snehil Chandra and Dhurata Stroni for all their support and being there with me, giving me a sense of home away from home. I also appreciate all the gratitude that my students gave me for being their TA. And lastly, I wish to thank Jesus for giving me the chance to come all the way here, for all the good things in life and most importantly giving me a chance to meet all these wonderful people.

Chapter 1

INTRODUCTION

1.1 Background and motivation

There has been a great amount of interest in recent years in the application of variable stiffness structures for semi-active structural control. Reference [**1**] shows that as early as the 90s, variable stiffness elements were used in telescoping axial truss members. When a piezoelectric actuator is placed on the contacts, the clamp between the two telescoping elements is released and the axial stiffness becomes close to zero. By extension of the piezoelectric actuator, the elements are clamped to each other and axial stiffness is restored. Reference [**2**] demonstrates a smart-spring concept. When a voltage is applied across the piezoelectric actuator, it generates a normal force that engages a secondary spring.

Semi-active control has been receiving a large amount of attention due to its ability to adapt to changing requirements utilizing very low power requirements. Gandhi and Anusonti examined the potential of using a semi-active controllable stiffness device whose spring constant can be modulated in real time for tonal disturbance rejection applications [**3**].

Stiffness variation can also be achieved using smart materials. Smart materials such as piezoelectric materials, Shape Memory Alloys (SMA) and Shape Memory Polymers (SMP) can be implemented in stiffness variation control systems. Researchers have demonstrated stiffness change through capacitive shunting [**4**] and state switching of piezoelectric materials [**5, 6**]. SMAs undergo austenite-martensite phase transformations with change in temperature. The elastic modulus in the austenite phase can be as much as 3 times greater than that in the martensite phase [**7, 8**].

SMAs have limited applications due to their high power consumption and slow operation. Lately, SMPs are becoming more popular due to their ability to display large changes in modulus and high strain capability at higher temperatures. In addition they can store strain and stiffen by orders of magnitude when cooled below the glass transition temperature [**9-11**]. Heating the polymer recovers the stored strain. References [**12**] and [**13**] report that variable stiffness elements are particularly interesting to morphing aircraft structures because load bearing structures in aircraft and rotorcraft need to be stiff under general operating conditions. Such structures would require a high morphing actuation force and power thus increasing power consumption costs. Research has been ongoing in the possibility of accomplishing shape or form change at low actuation costs and being able to revert to a high stiffness load bearing structure for normal operation.

Stiffness variations can be either per cycle or quasi-static. A piezoelectric material that is capactively shunted can undergo a rapid change in stiffness, but the magnitude of the stiffness change is relatively low. On the other hand, SMPs can undergo very large changes in stiffness. However in this case, the variation is stiffness is temperature driven and the bandwidth is relatively low. These systems would find applications in missions where quasi-static or slower variation in stiffness is required [**14**].

A chief motivation for this research is the recent experimental work conducted by Gandhi and Kang [**15**] on controllable flexural stiffness beams. They describe a method for controlling flexural stiffness of a multi-layered beam with aluminum base and cover layers. Sandwiched between these aluminum layers were 2 polymer layers embedded with heating pads. Figure **1-1** shows the experimental setup of a multi-layered beam. The flexural stiffness of the multi-layered beam is controlled via shear induced in the polymer layer through heating. Their results showed that the flexural bending stiffness of the beam reduced with increase in polymer temperature. At low temperatures, the flexural stiffness was found to be 2 to 4 times higher than at high temperatures as seen in Figure **1-2.**

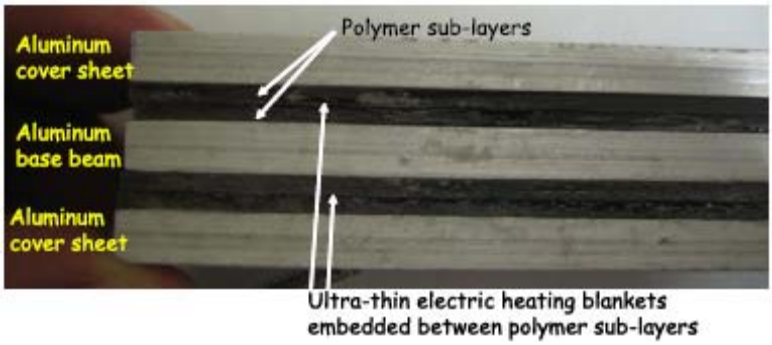

Figure **1-1**: Experimental Multi Layer Beam Setup [**15**]

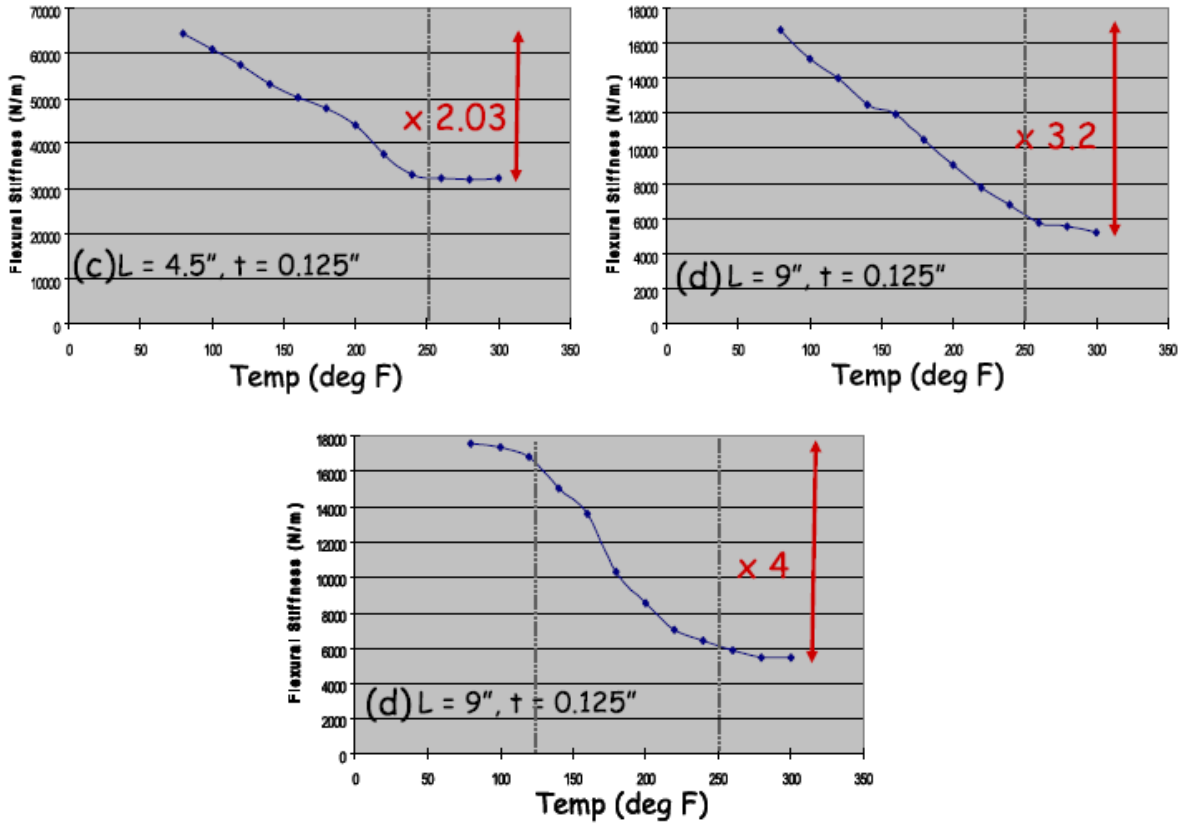

Figure **1-2**: Results of variation in beam flexural stiffness with temperature [**15**]

In addition to variable stiffness systems, the popularity of composite materials has increased exponentially over recent years. This is chiefly due to the design flexibility associated with composites. Also their superior performances compared to traditional metals have found them extensive use in aerospace engineering. More significantly, the ability to tailor composite materials to achieve the desired structural response has been widely documented over the past decades. Of particular significance is the ability to exploit the coupling that exists between various modes such as extension, bending, twisting and shear. Collectively, these are termed structural tailoring.

Structural tailoring is defined as the distribution of parameters such as stiffness, strength, etc. in a desired fashion to meet structural mission objectives. These parameters are highly dependent on choice of fiber, matrix, fiber orientation angle and number of plies in the laminate lay-up. To enable successful structural tailoring, it is important to identify the unique composite structural properties such as directionality and elastic couplings. References [**16-19**] analyze the effect of elastically coupled rotor blades on rotorcraft performance and stability. Extension-twist coupling (ETC) is considered to be the non-classical effect with the highest potential to optimize rotorcraft performance [**20**]. Although elastic tailoring has not been fully utilized in the design of modern composite rotor blades, it is recognized that elastic tailoring has the potential of significantly improving the aeroelastic performance of rotorcraft equipped with such blades over those equipped with conventional metal or composite blades. For this reason, elastic tailoring of composite rotor blades through specialized design of composite laminates has been a popular research topic in recent years.

Research has shown that composite designs which exhibit controllable elastic couplings can be used to reduce vibration, enhance aeroelastic stability and improve aerodynamic performance [**20**, **21**]. Reference [**22**] investigated the effects of non-classical behavior such as bending-shear coupling, torsion related out-of-plane warping and extension-twist coupling. Twist deformations shown are optimum for tiltrotor performance. Many studies have been conducted to quantify and validate the feasibility of elastic tailoring on composite beams with ETC. Lake et al [**23**] conducted research on passive blade twist control by varying the mass distribution along the blade length.

A significant amount of research [**24-26**] was conducted on elastic tailoring that involved coupling between extension, shear, torsion and bending. A large number of composite designs were developed. Carbon-epoxy was the most popular composite used. These designs were analyzed and validated with finite element models and experimental data. Various design variables such laminate stacking sequence, geometry of cross-section, number of plies, etc. were identified to tailor the structure for certain desired responses. Also, composite beam analysis done in [**27**] showed that the desired magnitude of twist can be achieved by the proper tailoring of composite laminates. Reference [**28**] proposed a sliding mass concept to provide significant additional flexibility to the structure in addition to the extension-twist coupling effects in real rotor blades.

The usefulness, practicality and extensive study of tailoring of composite material to control wing and blade performance were a major source of motivation for this research. However at the same time, the ever-increasing use of smart structures and materials in aerospace systems also was a motivational factor. The ability to actively, semi-actively and passively control structures stiffness through low energy consumption is a topic of interest in the recent years. These two widely applicable and advantageous concepts (composite couplings and variable stiffness structures) have not widely been explored in the same context on the same structure.

This thesis focuses on the quantification of couplings that exist in composite laminates. This is coupled with the concept of controlling beam stiffness by varying polymer stiffness in a multi-layered beam. Utilizing this method combines the advantages of using semi-active structures along with the exceptional extension-twist and bending-twist characteristics of composite materials.

1.2 Extension Twist Coupling and Bending Twist Coupling

Two of the significant couplings that exist in composite laminates include extension twist coupling (ETC) and bending twist coupling (BTC). In the case of ETC, the coupling effect is observed with an anti-symmetric stacking sequence (with respect to mid-plane) or lay-up of plies i.e. stacking $+\alpha$ and $-\alpha$ plies, where α is the ply angle orientation [**29**]. This is shown in Figure **1-3 .** An antisymmetric laminate undergoes antisymmetric shear deformation under an axially applied load. This action is equivalent to applying a couple in the axial direction resulting in an out-of-plane twist.

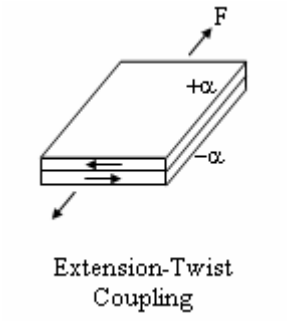

Figure **1-3**: Concept of Extension-Twist Coupling in Antisymmetric Lay-up Laminate

For a given set of material properties and geometry, the magnitude of this out-of-plane twist can be altered by varying the stacking sequence and ply angle. For an antisymmetric lay-up, the stiffness coefficients that determine the extension-twist coupling behavior are the axial stiffness, torsional stiffness and extension-twist coupling stiffness. Many manufacturing methods such as vacuum-bagging, filament winding and pre-preg can easily generate antisymmetry [**30**].

The Bending-Twist Coupling (BTC) effect is observed in laminates with symmetric lay-up of plies i.e. stacking $+\alpha$ and $+\alpha$ (or $-\alpha$ and $-\alpha$) plies as shown in Figure **1-4.** In this case, an applied bending moment causes an out-of-plane twist in the laminate. The BTC is highly enhanced when the laminate is unbalanced.

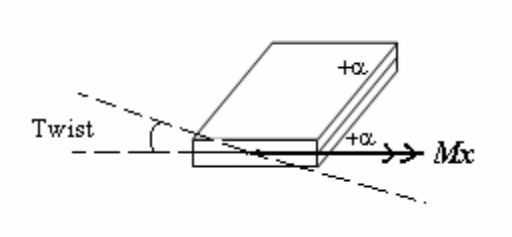

Figure **1-4**: Concept of Bending Twist Coupling in Laminates with Symmetric Lay-up

Similarly, for a given set of material properties and geometry, the magnitude of the twist can be altered by varying the stacking sequence and ply angle. The same fabrication methods can be used to manufacture symmetric laminates. For a symmetric lay-up, the stiffness coefficients that determine the bending-twist coupling behavior are the bending stiffness, torsional stiffness and the bending-twist coupling stiffness.

1.3 Objectives

The overall objective of this research is to explore the feasibility of controlled couplings of a composite multi-layer beam using polymer's thermal softening properties to decouple the system. The specific tasks are as follows:

1. Develop a set of metrics that will encapsulate the change in extension-twist and bending-twist coupling characteristics respectively, while ensuring sufficient stiffness in the beam's primary stiffness directions.
2. Perform studies of various laminate stacking sequences using the two theoretical extremes of the system, namely perfectly coupled and decoupled states.

3. Develop a finite element model of the multi-layer beam setup to include the shear effects of the polymer layer.
4. Computationally quantify the effects of a realistic polymer layer, namely the losses associate with the polymer's finite stiffness, stiffness range and thickness.

In this study, the multi-layered beam is simplified by using two plies as base layer and two outer plies as cover layers. Governing equations for extension, bending and torsion are derived using the Newtonian approach and the Classical Laminated Plate Theory [**29**]. A system of metrics is developed to capture the possible change in extension-twist as well as bending-twist coupling and to also ensure the beam's primary stiffness's are not drastically altered. The finite element model was developed and the analysis showed the extraction of the stiffness terms and coupling terms from the finite element model. The effect of the polymer layer is shown to decouple the system in the finite element model.

Chapter 2

DESCRIPTION OF APPROACH

This chapter begins with the physical description of the multi-layer beam setup used in this study. Appropriate lay-up designs are shown to quantify the extension-twist and bending-twist coupling effects. The detailed description of the concept of stiffness variation through change in shear modulus of the polymer layer to decouple the system is described. Constraints on extensional and bending stiffness' are used to develop the metrics for the extension-twist and bending-twist effects respectively.

2.1 Description of Beam Setup

Reference [**15**] described an experimental setup for variation of beam flexural stiffness. A similar concept was employed in this study. Figure **2-1** shows a schematic of the setup of a multi-layered beam. The scale has been greatly magnified to show the various layers. The beam is clamped at the left end and free at the right end. This composite beam consists of two inner plies having a certain known elastic coupling by virtue of their ply orientation. This is referred to as the base layer and is indicated in green in Figure **2-1**. On the top and bottom of these plies, there is a thin polymer layer with known stiffness. The thickness of the polymer layers is less than that of the ply thickness. An ultra-thin heating pad is embedded in the polymer layers. The application of these heating pads is discussed later.

This structure was then sandwiched between two composite plies, one on the top and one on the bottom respectively bonded to the polymer layer. These two outer plies are referred to as cover layers. They are indicated in yellow in Figure **2-1**. The thickness of the outer ply and inner ply were the same for the simulations in this study. Figure **2-2**

shows the same setup in an exploded view. Here the outer ply angles (relative to the 0° fiber orientation) are denoted as **α** and the inner ply angles are denoted as **θ**. The thickness of the plies is indicated by ***t***. The multi-layered beam is symmetric about the mid-plane.

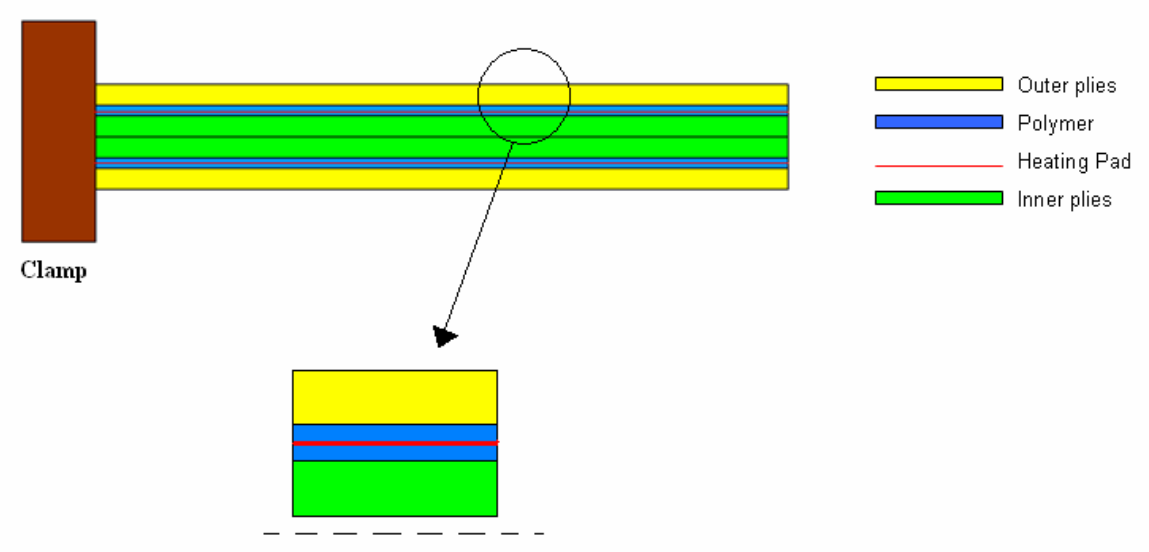

Figure **2-1**: Schematic Representation of Multi-layered Beam

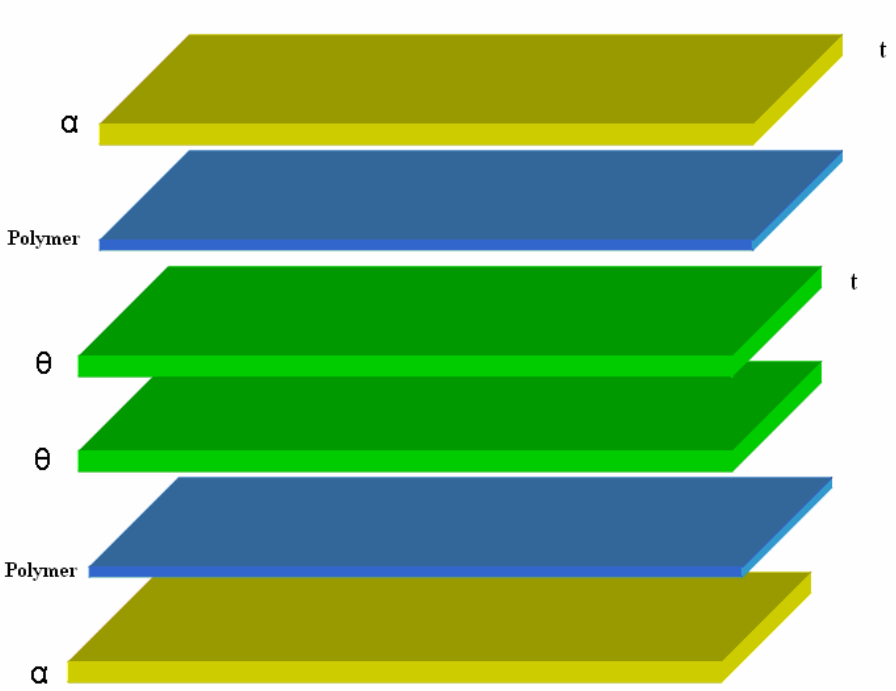

Figure **2-2**: Multi-beam lay-up exploded view

2.2 Description of Stiffness Variation Mechanisms

When subject to extensional and bending loads, the deformation mode of the multi-layered beam depends significantly on the shear modulus of the polymer layer in conjunction with the coupling mechanics of the base beam and cover layers. Many polymers' stiffness are dependent on temperature. The shear modulus of a typical polymer reduces significantly with increase in temperature. Polymers can be found whose shear modulus reduces by up to 3 orders of magnitude upon increase in temperature. Figure **2-3** [**15**] shows this characteristic for two different commercially available polymers. At lower temperatures, the shear modulus of the polymer layer is high. In this state, the polymer is in the "glassy" state. As can be seen in Figure **2-3**, as the temperature increases, the polymer goes through its glass transition and there is a rapid decrease in shear modulus. At higher temperatures, the polymer's state is in the "rubbery" and its shear modulus being several orders of magnitude lower than the "glassy" modulus.

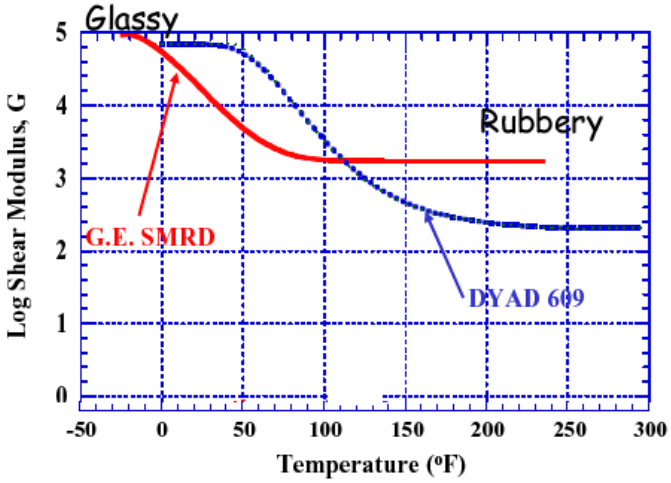

Figure **2-3**: Typical Variation of Shear Modulus with Temperature Increase [**15**]

When the polymer layer is in the glassy state, i.e. its shear modulus G is high; the deformation of the beam under bending load is shown in Figure **2-4**. The stiff cover layers are coupled to the base layers. Thus the beam behaves as an integral unit. In effect,

as a composite laminate, the multi-layered beam acts as a 4 ply laminate exhibiting all the couplings associated with the particular ply orientation in the lay-up. Thus the displacements and strains due to the application of the external load is dominated by all four plies in the laminate. The system also has a higher bending and extensional stiffness due the effect of the four plies. Figure **2-4** (a) shows the side view of the beam under an extensional and bending force. (b) shows a close up of the layers showing the stiff polymer layers. This leads to the beam behaving as an integral unit. (c) shows the twist induced due to the elastic couplings.

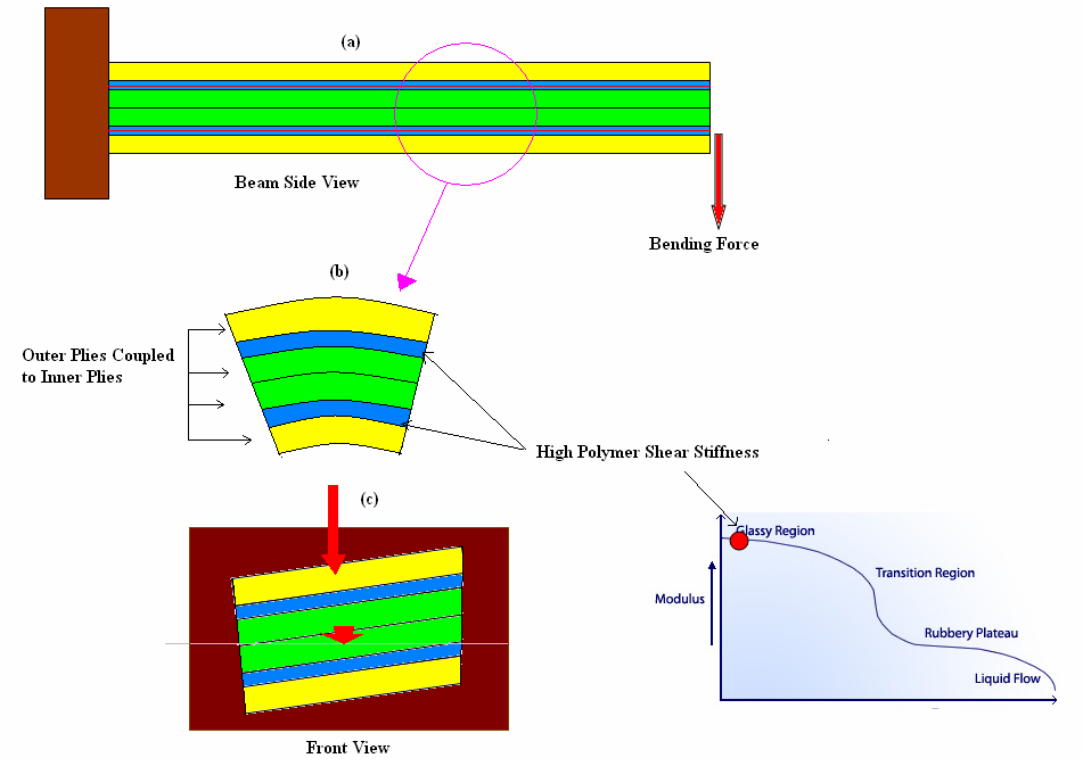

Figure **2-4**: Stiff Polymer (a) Side view of beam under Extensional and Bending Loads, (b) Schematic of coupled ply and polymer layers, (c) Front view of beam tip twist

If an ultra-thin Kapton electric heating pad [**15**] is embedded in the polymer layers and the temperature can be controlled and monitored, the shear stiffness of the polymer can be varied. Thus by increasing the temperature, the shear modulus can be lowered significantly (by up to 3 orders of magnitude). With a low shear modulus

polymer layer, the multi-layered beam deforms as depicted in Figure **2-5** under the same bending load as before. Now in this case, the outer plies act like a constraining layer, thereby inducing shear in the polymer layer. As can be seen in Figure **2-5**, the shear deformation in the polymer layer effectively decouples the inner plies from the outer plies, and now the overall stiffness and structural couplings are largely dependent on the inner plies. Thus the coupling behavior associated with the ply orientation of the inner layers begins to dominate the beam's displacement.

In the case when the polymer was stiff, all the plies contributed to the beam stiffness and structural couplings. Now with a soft polymer layer, the contribution to stiffness is mainly from the inner plies. It is thus clear that the overall stiffness and coupling behavior of the multi-layered beam can be controlled if the shear modulus of the intermediate compliant polymer layer could be varied by a temperature controller.

Similar to Figure **2-4**, the deformation of the beam is shown under a bending load in Figure **2-5**. When the polymer is soft, the close up of the layers is also seen wherein the low stiffness polymer layer essentially decouples the inner plies from the outer plies. The deformations produced are greater since the behavior of the laminate is dominated by the two inner plies.

This concept of controlling the beam couplings can be advantageous to many structural systems. It should be noted that as the outer plies are decoupled from the base beam, the primary beam stiffness's (flexural, extensional and torsional) would also reduce. One of the goals in this study is to maximize the change in coupling while limiting the change in primary stiffness. In the following section, the appropriate numerical metrics are developed to achieve this stated objective.

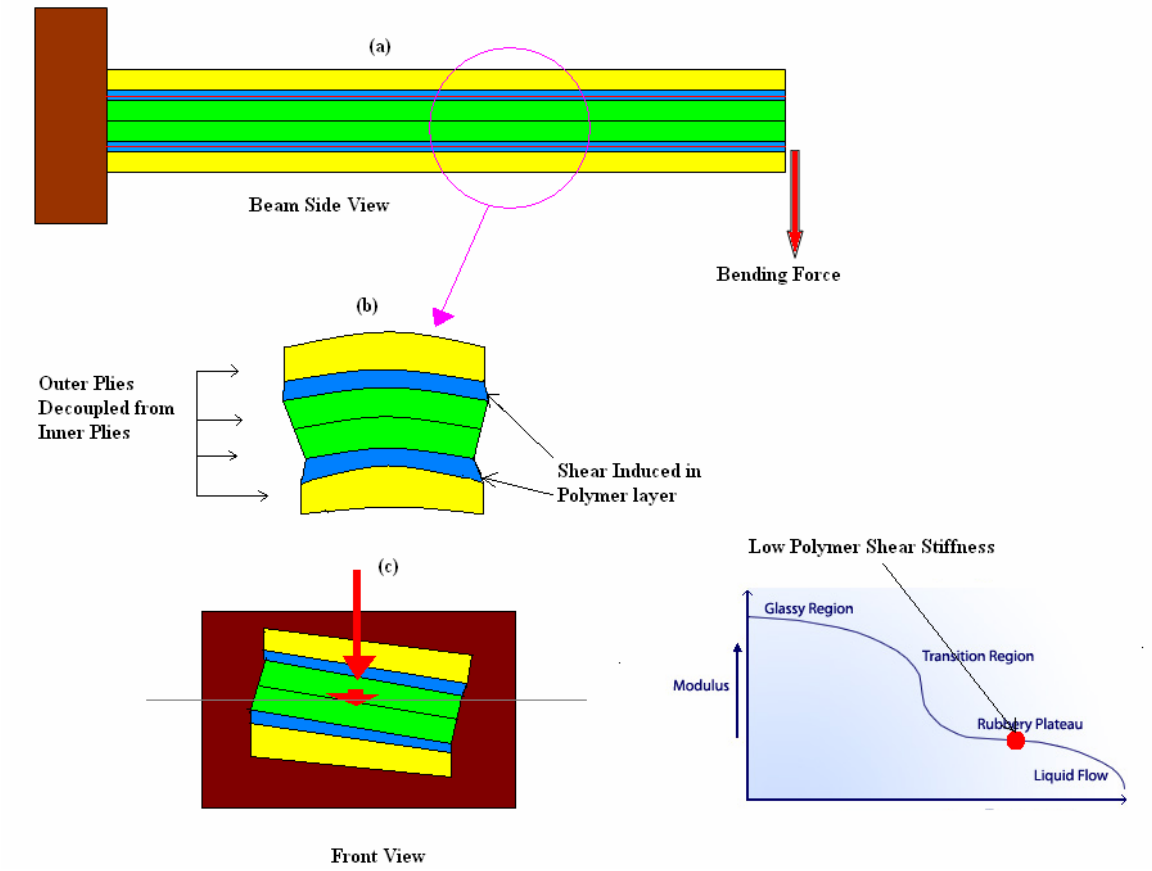

Figure **2-5**: Soft Polymer (a) Side view of beam under Extensional and Bending Loads, (b) Schematic of decoupled ply and polymer layers, (c) Front view of beam tip twist

2.3 Development of Metrics

The design of a multi-layered beam with elastic couplings that can undergo a large variation using the concepts described in section 2.2 is easier to accomplish when the beam is structurally soft. However such a beam would be unable to carry structural loads. A beam that is capable of undergoing large changes in structural coupling but is unsuitable for use as a load bearing structure would have very limited value. As a result, metrics were established to quantify the change of elastic couplings without the loss of structural stiffness of the beam.

In particular, this study focuses on the Classical Laminate Plate Theory (CLPT), for a perfectly bonded laminate lay-up consisting of plies with varying ply angle orientations respectively, the terms that represent the Extension-Twist Coupling (ETC) and Bending-Twist Coupling (BTC) are B_{16} and D_{16} respectively. The extensional stiffness is A_{11}, the bending stiffness is D_{11} and the torsional stiffness is D_{66}.

2.3.1 Extension-Twist Metric (ETM)

A composite beam that has an anti-symmetric lay-up with respect to its mid plane displays Extension-Twist Coupling (ETC). On application of an axial extensional force only to the free end of the beam (Figure **2-6)**, the expression relating force/moment resultants to strain/curvatures reduces to Equation **2.1**. Refer to Appendix **A** for definition of terms and derivation of equations.

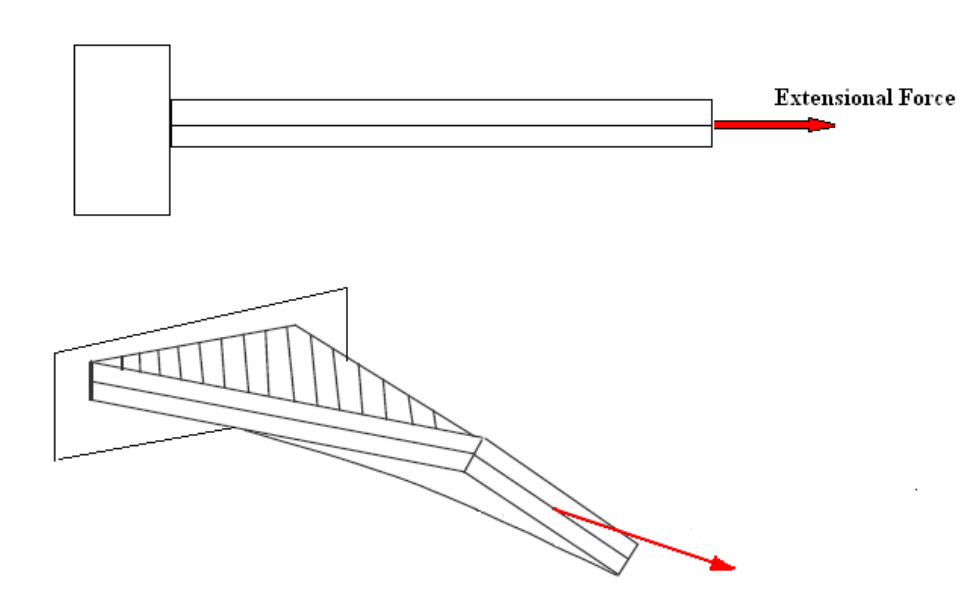

Figure **2-6**: Application of Axial Extensional Force

$$\begin{Bmatrix} N_x \\ M_{xy} \end{Bmatrix} = \begin{bmatrix} A_{11} & B_{16} \\ B_{16} & D_{66} \end{bmatrix} \begin{Bmatrix} \varepsilon_x \\ \kappa_{xy} \end{Bmatrix} \qquad \text{(Eq. 2.1)}$$

Thus in Equation **2.1**, the stiffness terms are A_{11} and D_{66}. These refer to the extensional and torsional stiffness respectively. The B_{16} term is the main coupling term. The goal is to maximize the change in coupling between the 4-ply coupled state B_{16}^{4ply} and the 2-ply decoupled state B_{16}^{2ply}. Thus effectively the coupled state refers to all 4 plies contributing to the coupling effects and the decoupled state refers to just the coupling effects from the two inner plies. The outer plies are decoupled from the system.

Based on the above criteria, a metric needs to be developed with the following requirements simultaneously:

1. The difference in coupling between the four-ply state and two-ply state ($B_{16}^{4ply} - B_{16}^{2ply}$) is to be maximized.
2. The change in extensional stiffness (A_{11}^{4ply} and A_{11}^{2ply}) is to be minimized.
3. The change in torsional stiffness (D_{66}^{4ply} and D_{66}^{2ply}) is also to be minimized.
4. The average extensional and torsional stiffness of the beam structure should be maintained. (It is not desired to have a structural coupling that is low in extensional and bending stiffness).

Equation **2.2** shows a metric developed to meet the above requirements. This metric is referred to as the Extension Twist Metric (ETM)

$$\text{Extension - Twist Metric} \quad (\text{ETM}) \quad = \quad \frac{\left|B_{16}^{2ply} - B_{16}^{4ply}\right|\left(A_{11}^{2ply} + A_{11}^{4ply}\right)\left(D_{66}^{2ply} + D_{66}^{4ply}\right)}{\left|A_{11}^{2ply} - A_{11}^{4ply}\right|\left|D_{66}^{2ply} - D_{66}^{4ply}\right|} \qquad \text{(Eq. 2.2)}$$

The numerator of the ETM contains the difference in coupling between the coupled (4-ply) and decoupled (2-ply) system. Also in the numerator are the mean extensional and torsional stiffness of the coupled and decoupled states. The numerator attempts to maximize the change in ETC between the coupled and decoupled states while simultaneously maintaining an acceptable mean value of the primary extensional and

torsional stiffness of the beam in the coupled and decoupled states. The denominator contains differences in the extensional and torsional stiffness between coupled and decoupled states. The denominator in the ETM ensures against excessive change in the beam's primary extensional and torsional stiffness between the coupled and decoupled states. Thus a high value of the ETM implies that the beam exhibits a good change in ETC but continues to be viable as a load bearing structure.

Thus the maximum value of the ETM is used as a parameter in obtaining the ply angle orientation and lay-up of inner and outer plies.

2.3.2 Bending Twist Metric (BTM)

A composite has that symmetric lay-up with respect to its mid-plane displays Bending-Twist Coupling (BTC). Application of a bending moment to the free end of the beam (Figure **2-7**), the expression relating force/moment to the strains/curvatures reduces to Equation **2.3**. Refer to Appendix **A** for definition of terms and derivation of equations.

In the case of bending moment applied as in Equation **2.3**, the stiffness terms are D_{11} and D_{66}. These refer to the bending and torsional stiffness respectively. Here the D_{16} term is the main coupling term. As in the case of the ETM, the goal is to maximize the change in coupling between the 4-ply coupled state D_{16}^{4ply} and the 2-ply decoupled state D_{16}^{2ply}. Thus effectively the coupled state refers to all 4 plies contributing to the coupling effects and the decoupled state refers to just the coupling effects from the two inner plies. The outer plies are decoupled from the system.

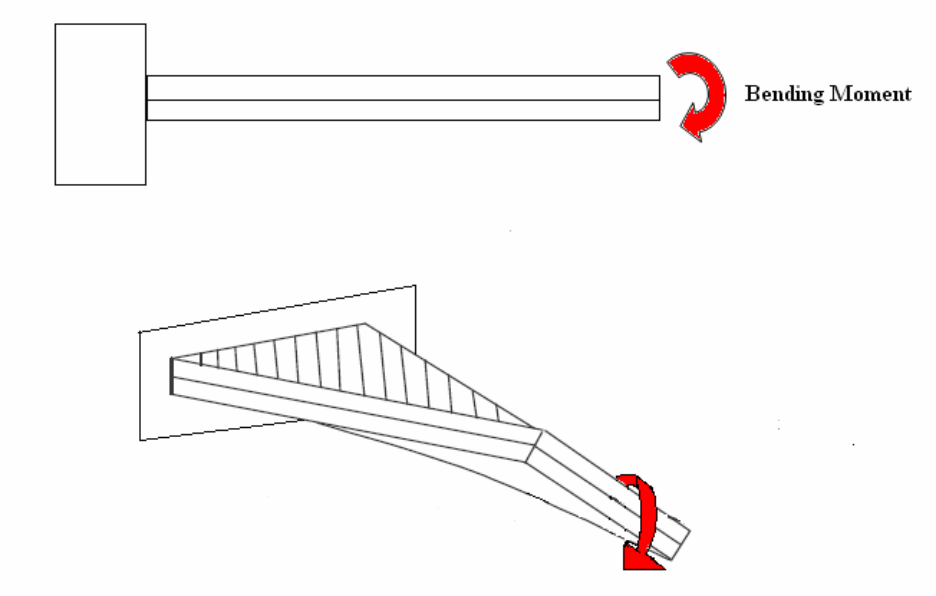

Figure **2-7**: Application of Bending Moment

$$\begin{Bmatrix} M_x \\ M_{xy} \end{Bmatrix} = \begin{bmatrix} D_{11} & D_{16} \\ D_{16} & D_{66} \end{bmatrix} \begin{Bmatrix} \kappa_x \\ \kappa_{xy} \end{Bmatrix} \qquad \text{(Eq. } \mathbf{2.3}\text{)}$$

In the case of bending moment applied as in Equation **2.3**, the stiffness terms are D_{11} and D_{66}. These refer to the bending and torsional stiffness respectively. Here the D_{16} term is the main coupling term. As in the case of the ETM, the goal is to maximize the change in coupling between the 4-ply coupled state D_{16}^{4ply} and the 2-ply decoupled state D_{16}^{2ply}. Thus effectively the coupled state refers to all 4 plies contributing to the coupling effects and the decoupled state refers to just the coupling effects from the two inner plies. The outer plies are decoupled from the system.

Based on the above criteria, a metric needs to be developed with the same requirements as outlined in the ETM case. However the major difference is that the concern at present is with the conservation of the bending stiffness and not the extensional stiffness. Equation **2.4** shows the metric developed to meet the requirements of large change in bending-twist coupling while minimizing the change in the bending and torsional stiffness. This metric is referred to as the Bending Twist Metric (BTM).

$$\text{Bending} - \text{Twist Metric } (BTM) = \frac{\left|D_{16}^{2\,ply} - D_{16}^{4\,ply}\right|\left(D_{11}^{2\,ply} + D_{11}^{4\,ply}\right)\left(D_{66}^{2\,ply} + D_{66}^{4\,ply}\right)}{\left|D_{11}^{2\,ply} - D_{11}^{4\,ply}\right|\left|D_{66}^{2\,ply} - D_{66}^{4\,ply}\right|} \qquad \text{(Eq. } \mathbf{2.4}\text{)}$$

The numerator of the BTM contains the difference in coupling between the coupled (4-ply) and decoupled (2-ply) system. Also in the numerator are the mean bending and torsional stiffness of the coupled and decoupled states. The numerator attempts to maximize the change in BTC between the coupled and decoupled states while simultaneously maintaining an acceptable mean value of the primary bending and torsional stiffness of the beam in the coupled and decoupled states. The denominator contains differences in the bending and torsional stiffness between coupled and decoupled states. The denominator in the BTM ensures against excessive change in the beam's primary bending and torsional stiffness between the coupled and decoupled states. Thus a high value of the BTM implies that the beam exhibits a good change in BTC but continues to be viable as a load bearing structure.

Thus the maximum value of the BTM is used as a parameter in obtaining the ply angle orientation and lay-up of inner and outer plies. The ensuing analysis details the methods of obtaining the maximum values of the ETM and BTM respectively by using various combination of inner and outer ply angle orientation. Models used in the numerical calculation of the metrics are presented in Chapter **3**.

Chapter 3

MODELING

This chapter begins with the description of the physical dimensions of the multi-layered beam along with a description of the material properties used. Two different analytical models are used in this study. The first model is in Matlab and assumes perfect bonding between layers ignoring the effect of the polymer layer. The second model is used ANSYS finite element software and explicitly represents the polymer layers between the base beam and the outer layers so that the strain transfer through shear in the polymer layer is properly depicted. Both models calculate the ETM and BTM values for various ply angle orientations.

3.1 Dimensions and Material Properties

As seen in Figure **3-1** , the length of the beam ***L*** is chosen as 25.4 cm. The width ***b*** is 5.08 cm. The thickness of each ply **t** is 0.5 mm. The ply angle of the inner plies is denoted as $\boldsymbol{\theta}$ and the ply angle of the outer plies is denoted as $\boldsymbol{\alpha}$. When $\alpha = \theta = 0°$, the fibers run along the length of the beam. The dimensions were chosen based upon the dimensions of available heating pads embedded in between the polymer layers. These parameters are summarized in Table **3-1.**

Table **3-1**: Summary of Beam Dimensions

Dimension	**Value**
Length (L)	25.4 cm
Width (b)	5.08 cm
Ply thickness (t)	0.5 mm

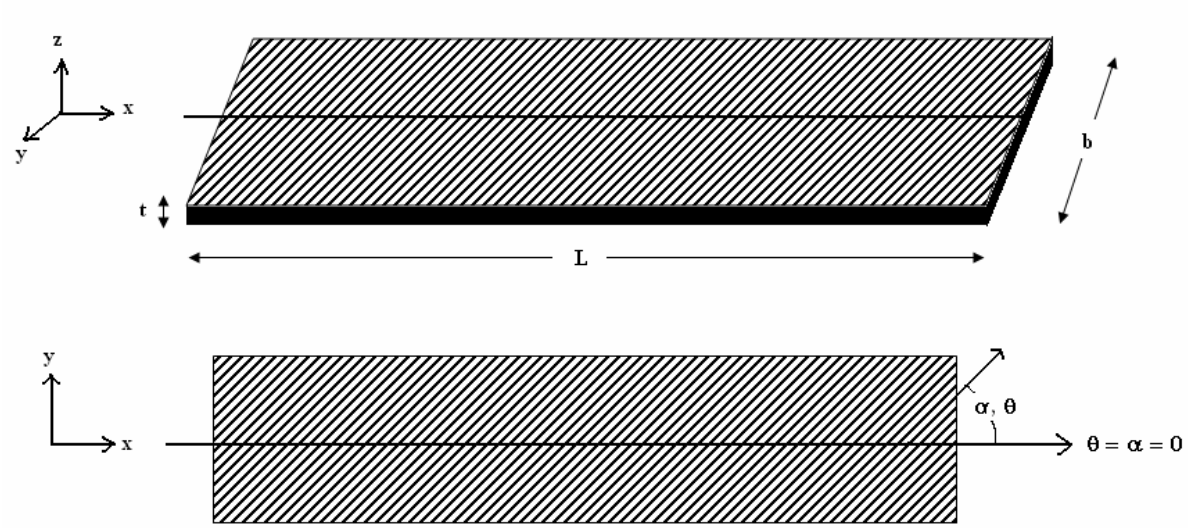

Figure **3-1**: Beam Dimensions and Coordinate System

The material chosen for the composite plies was Graphite/Epoxy (Gr/E). This material consists of carbon (graphite) fibers in a standard epoxy matrix. This material is commonly used in structural load bearing systems and thus was an ideal choice in this analysis. The Young's modulus in the fiber (E_L) direction is about 15 times that in the matrix (E_T) direction. Material properties were chosen for the polymer layer, such that upon heating, the transition from the stiff glassy state to the soft rubbery state lowers the shear modulus of the polymer by three orders of magnitude. At this point the thickness of the polymer layer is left as a variable with the only constraint that it cannot be thicker than the individual ply layers. Table **3-2** summarizes the composite properties along with the polymer properties; the "*x*" in the polymer thickness column indicates that this value is a variable which will be calculated later. Values displayed in the table are standard values for Gr/E composite with a 0.55 volume fraction.

Table **3-2**: Material Properties

Material	E_L	E_T	G_{LT}	v_{LT}	t
Gr/E Composite	138	8.96	7.89	0.32	0.5
Polymer (Glassy State)	29	29	10	0.45	x
Polymer (Rubbery State)	29 x 10^{-3}	29 x 10^{-3}	10 x 10^{-3}	0.45	x

These material properties will be used in the following Matlab and Finite Element model.

3.2 MATLAB Model

When the effect of the bond layer is not considered, the behavior of a 2-layer laminate (inner θ plies only) and 4-layer laminate (inner θ and outer α plies) can be analyzed quickly and easily. Using the 2-layer and 4-layer laminate (without the polymer layer) in the calculation of the ETM and BTM establishes the limits (maximum values) on these metrics. In other words, if the outer α plies could be *completely* decoupled from the inner θ plies, how much change in ETC or BTC would be possible? When the effect of the polymer layer is accounted for, neither would the outer plies be completely coupled to the inner plies when the polymer is glassy, nor would they be completely decoupled when the polymer is rubbery. So the metrics calculated using a 2-layer and a 4-layer beam without the polymer represent the largest changes in couplings possible. This model uses the following simplifying assumptions:

1. Classic Laminated Plate Theory (CLPT) is used to model the ply layers in the multi-layered beam.
2. The presence of the polymer layer is not considered since the CLPT cannot model the shear mechanics of the polymer layer.

3. Perfect bonding between layers is assumed. This represents a bond which is infinitesimally small and non-shear deformable. So the outer plies are perfectly coupled to the inner plies.
4. It is assumed that the system can be completely decoupled to the effect that the outer two plies are virtually absent in the decoupled case.
5. The polymer layer is not modeled, but it is assumed that it is the reduction in the shear modulus of the polymer that decouples the system.

Thus under these perfect conditions, the multi-layered beam can be modeled separately as a 4-ply and 2-ply system in the coupled and decoupled states respectively. Appendix **B** contains the details of the Matlab program.

Initially the 4 ply coupled system is considered. Table **3-3** lists the various input and output parameters used in the Matlab analysis for computation of the ETM. In the ETM analysis, the ply lay-up was anti-symmetric as shown in Figure **3-2**. Anti-symmetric lay-ups produce extension twist coupling. The inner ply angle was varied from 0° to 90° in increments of 15°. The outer ply angle was varied from -90° to 90° in increments of 15°.

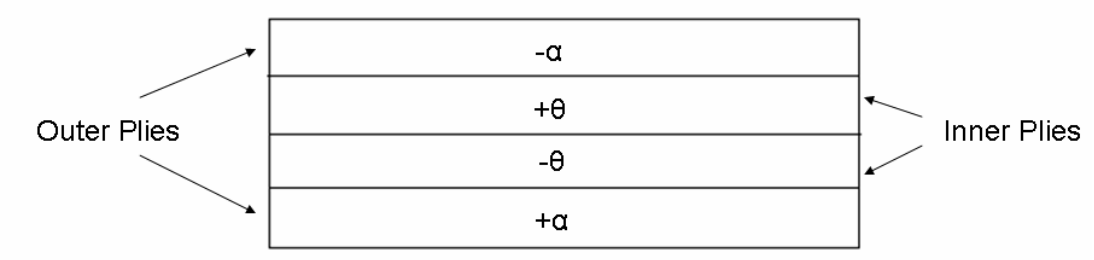

Figure **3-2**: Anti-symmetric Lay-up

Table **3-3**: Input and Output Parameters from Matlab Model

Input	• Ply angle Orientations α=[-90, 90], θ =[0, 90] • Material Properties E_L, E_T, G_{LT}, ν_{LT}. • Dimensions L, b, t
Output	• A, B, D matrices.

Knowing the terms of the A, B and D matrices, the terms B_{16}^{4ply} , A_{11}^{4ply} and D_{66}^{4ply} can be obtained. The above analysis is repeated but this time a perfectly decoupled system consisting of just the two plies is modeled. Thus the program now inputs only values of [θ/-θ] as its two plies in the laminate. From this output, the A, B, D matrices are obtained if the outer plies can be completely decoupled. Consequently, the B_{16}^{2ply}, A_{11}^{2ply} and the D_{66}^{2ply} are obtained. Equation **3.1** recalls the ETM expression. It is clear that all terms in this equation are obtained from the Matlab analysis to give a numerical value for the ETM.

$$\text{Extension - Twist Metric} \quad (\text{ETM}) \quad = \quad \frac{\left|B_{16}^{2ply} - B_{16}^{4ply}\right|\left(A_{11}^{2ply} + A_{11}^{4ply}\right)\left(D_{66}^{2ply} + D_{66}^{4ply}\right)}{\left|A_{11}^{2ply} - A_{11}^{4ply}\right|\left|D_{66}^{2ply} - D_{66}^{4ply}\right|} \qquad \text{(Eq. 3.1)}$$

Similarly, the program was run again for the calculation of the BTM. The inputs and outputs are the same as described in Table 3-2 but the laminate stacking sequence is symmetric as shown in Figure **3-3.** The inner ply angle was varied from 0° to 90° in increments of 15°. The outer ply angle was varied from -90° to 90° in increments of 15°.

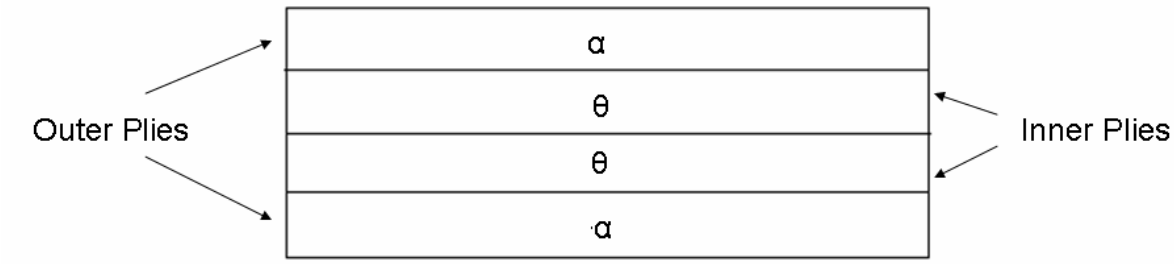

Figure **3-3**: Symmetric Layup

The program again outputs the A, B and D matrices for the 4-ply coupled state. From this, the values of D_{16}^{4ply} , D_{11}^{4ply} and D_{66}^{4ply} are obtained. For the perfectly decoupled case, the existence of only two inner plies is modeled and the corresponding A, B and D matrices are again obtained. From this two ply stiffness matrices, the D_{16}^{2ply}, D_{11}^{2ply} and the D_{66}^{2ply} terms are obtained.

Recalling the BTM expression in Equation **3.2** , it can be clearly seen that all terms of the expression are obtained and thus the BTM value can be calculated.

$$\text{Bending} - \text{Twist Metric } (BTM) = \frac{\left|D_{16}^{2ply} - D_{16}^{4ply}\right|\left(D_{11}^{2ply} + D_{11}^{4ply}\right)\left(D_{66}^{2ply} + D_{66}^{4ply}\right)}{\left|D_{11}^{2ply} - D_{11}^{4ply}\right|\left|D_{66}^{2ply} - D_{66}^{4ply}\right|} \qquad \text{(Eq. 3.2)}$$

The Matlab model provides the values of the ETM and BTM that can be achieved for a perfectly decoupled system and without the presence of the polymer layers. This gives a good estimate of the limiting value of the ETM and BTM that can be obtained. However, the assumptions used in the Matlab model do not always hold true in the presence of a finite thickness and finite stiffness polymer layer. Also the presence of the polymer layer does not allow the system to be either perfectly coupled or completely decoupled. The following section describes the development of a finite element model to capture the shear mechanics of the polymer layer in the multi-layered beam setup.

3.3 ANSYS Model

A finite element model of the multi-layered beam is also developed using the ANSYS software. The advantage of employing ANSYS is that through finite element analysis, the effect of the polymer layers can be properly included in the beam model. Thus the shear kinematics of the polymer layer can be captured and more accurate depiction of the coupling and decoupling behavior associated with the composite multi-layered laminate is represented. This model also shows the presence of the polymer layer as a coupling/decoupling medium for the system. The extent of the couplings is limited by the presence of the polymer.

The finite element model is able to input the beam dimensions and ply orientations. The necessary boundary conditions can be imposed. In this case, one end is clamped and the other end is acted upon by an axial extensional load or an applied bending moment, respectively. The model can output the values of strains and displacements. The polymer modulus can be adjusted for calculating the responses under loading and the stiffness and elastic coupling properties in the stiff state and soft state respectively. This will in turn enable the calculation of the ETM and BTM respectively. Table **3-4** summarizes the input and output parameters of the ANSYS model.

Table **3-4**: Input and Output Parameters for the ANSYS model

Input	• Ply angle Orientations α=[-90, 90], θ =[0, 90] • Material Properties E_L, E_T, G_{LT}, ν_{LT}. • Beam and ply dimensions L, b, t • Polymer properties E, G, ν • Axial extension Load N_{xx}, Bending Moment M_{xx} and Torsional Moment M_{xy}
Output	• Axial Strain • u_x, u_y, u_z displacements

To model the beam accurately, ANSYS provides various structural elements each having their own modeling features and constraints. In this analysis, the SOLID 45 element was used to model the composite ply and polymer layers. This element is used for the solid modeling of three dimensional structures. It is defined by eight nodes having three degrees of freedom at each node: translations in the nodal x, y, and z directions. This element also has plasticity, large deflection and large strain capabilities. Figure **3-4** with reference from [**31**] shows the geometry, node locations and coordinate systems for the SOLID 45 element. This element has orthotropic material properties with the direction corresponding to element coordinate directions. This element can output nodal solutions as well as other outputs such as stress and strain.

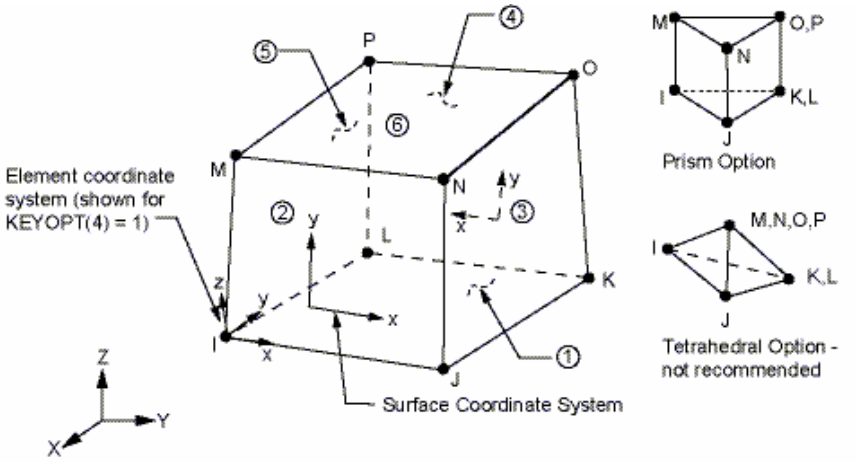

Figure **3-4**: SOLID 45 Geometry [**31**]

3.3.1 Extraction of Terms in the ETM

The ETM expression is shown in Equation **3.1**. In the ANSYS model, the perfect 4-ply and 2-ply cases cannot be assumed. Thus from this point onwards, the 4-ply system is referred to as "coupled' and the 2-ply system is referred to as "decoupled". From Equation **3.1**, it is clear that the outputs of the ANSYS model should enable the calculation of the A_{11}, B_{16} and D_{66} terms in the coupled and decoupled state.

On application of an axial extensional force only to the free end of the beam, the Force Resultant Matrix reduces to Equation **3.3** . Refer to Appendix **A** for definition and derivation of terms.

$$\begin{Bmatrix} N_{xx} \\ M_{xy} \end{Bmatrix} = \begin{bmatrix} A_{11} & B_{16} \\ B_{16} & D_{66} \end{bmatrix} \begin{Bmatrix} \varepsilon_{xx} \\ \kappa_{xy} \end{Bmatrix} \qquad \text{(Eq. 3.3)}$$

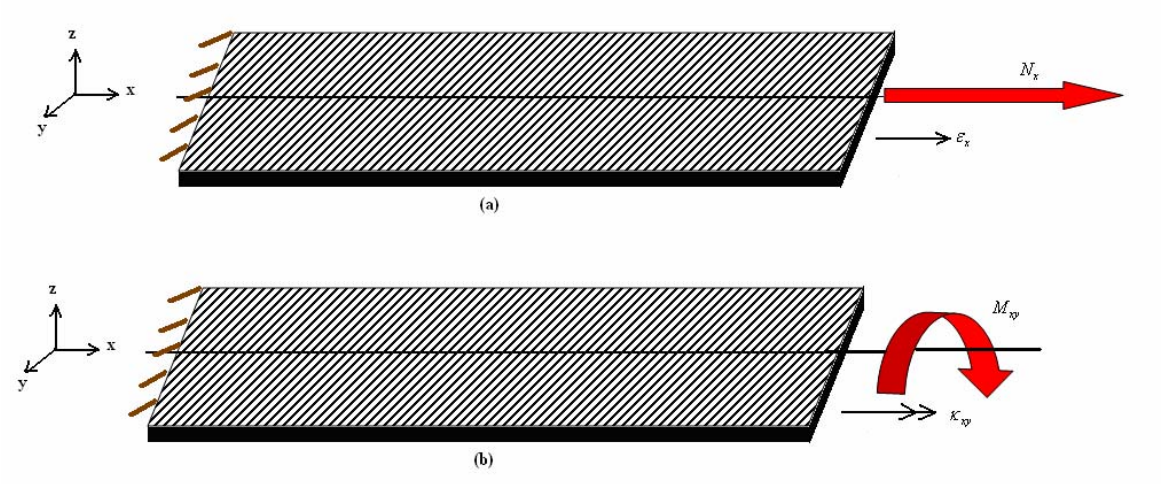

Figure **3-5**: Beam Applied Forces and Moments

As seen in Figure **3-5**, $\mathbf{N_{xx}}$ is the axial force in the x-direction. $\mathbf{M_{xy}}$ is the applied torque. $\boldsymbol{\varepsilon_{xx}}$ and $\boldsymbol{\kappa_{xy}}$ refer to the axial strain and twist curvature respectively. As seen in Figure **3-5 (a)**, if only a known extension force N_{xx} and no torque (M_{xy}) is applied to the beam, Equation 3.3 reduces to Equation **3.4** .

$$\begin{Bmatrix} N_{xx} \\ 0 \end{Bmatrix} = \begin{bmatrix} A_{11} & B_{16} \\ B_{16} & D_{66} \end{bmatrix} \begin{Bmatrix} \varepsilon_{xx} \\ \kappa_{xy} \end{Bmatrix} \qquad \text{(Eq. } \mathbf{3.4}\text{)}$$

By imposing a known external force N_{xx} on the beam, the values of $\boldsymbol{\varepsilon_{xx}}$ and $\boldsymbol{\kappa_{xy}}$ can be obtained from the ANSYS output. Thus Equation **3.4** can be written as shown in Equation **3.5** and Equation **3.6** :

$$N_{xx} = A_{11}\varepsilon_{xx} + B_{16}\kappa_{xy} \qquad \text{(Eq. } \mathbf{3.5}\text{)}$$

$$0 = B_{16}\varepsilon_{xx} + D_{66}\kappa_{xy} \qquad \text{(Eq. } \mathbf{3.6}\text{)}$$

Solving Equation 3.6 gives Equation **3.7**. Substituting Equation 3.7 in Equation 3.5 gives Equation **3.8**.

$$B_{16} = -\frac{D_{66}\kappa_{xy}}{\varepsilon_{xx}} \qquad \text{(Eq. } \mathbf{3.7}\text{)}$$

$$N_{xx} = A_{11}\varepsilon_{xx} - D_{66}\frac{\kappa_{xy}^2}{\varepsilon_{xx}} \qquad \text{(Eq. } \mathbf{3.8}\text{)}$$

In Equation 3.8, assume the following

$$\frac{\kappa_{xy}^2}{\varepsilon_{xx}} = K_1$$

Substituting this value of K_1 in Equation 3.8 gives Equation **3.9**.

$$N_{xx} = A_{11}\varepsilon_{xx} - D_{66}K_1 \qquad \text{(Eq. } \mathbf{3.9}\text{)}$$

In Equation 3.9, N_{xx}, $\boldsymbol{\varepsilon_{xx}}$ and K_1 are known quantities that can be obtained from the ANSYS solution. Thus in this equation, A_{11} and D_{66} are the variables.

In the same beam, if only a known external torque M_{xy} is applied as shown in Figure **3-5 (b)**, in absence of an axial force Equation **3.3** reduces to Equation **3.10**

$$\begin{Bmatrix} 0 \\ M_{xy} \end{Bmatrix} = \begin{bmatrix} A_{11} & B_{16} \\ B_{16} & D_{66} \end{bmatrix} \begin{Bmatrix} \varepsilon_{xx} \\ \kappa_{xy} \end{Bmatrix} \qquad \text{(Eq. } \mathbf{3.10}\text{)}$$

By imposing a known external torque M_{xy} on the beam, corresponding values of $\boldsymbol{\varepsilon_{xx}}$ and $\boldsymbol{\kappa_{xy}}$ can be obtained. Thus Equation **3.10** can be written as shown in Equation **3.11** and Equation **3.12** :

$$0 = A_{11}\varepsilon_x + B_{16}\kappa_{xy} \qquad \text{(Eq. } \mathbf{3.11}\text{)}$$

$$M_{xy} = B_{16}\varepsilon_{xx} + D_{66}\kappa_{xy} \qquad \text{(Eq. } \mathbf{3.12}\text{)}$$

Solving Equation 3.11 gives Equation **3.13**. Substituting Equation 3.13 into Equation 3.12 gives Equation **3.14**.

$$B_{16} = -\frac{A_{11}\varepsilon_{xx}}{\kappa_{xy}} \qquad \text{(Eq. } \mathbf{3.13}\text{)}$$

$$M_{xy} = -\frac{A_{11}\varepsilon^{2}{}_{xx}}{\kappa_{xy}} + D_{66}\kappa_{xy} \qquad \text{(Eq. } \mathbf{3.14}\text{)}$$

In Equation 3.14, assume:

$$\frac{\varepsilon_{xx}^{2}}{\kappa_{xy}} = K_2$$

Substituting this value of K_2 in Equation 3.14 gives Equation **3.15**.

$$M_{xy} = D_{66}\kappa_{xy} - A_{11}K_2 \qquad \text{(Eq. } \mathbf{3.15}\text{)}$$

In Equation 3.15, M_{xy}, K_2 and κ_{xy} are known quantities obtained from the ANSYS solution. Note that the values of κ_{xy} and ε_{xx} obtained in Equations 3.9 and 3.15 are different since Equation 3.9 was obtained under application of an external axial force only and Equation 3.15 was obtained under application of an applied torque only.

Equations 3.9 and 3.15 are two equations in two variables (unknowns) i.e. A_{11} and D_{66}. All other terms are known. Thus, the values of A_{11} and D_{66} can be calculated by solving Equations 3.9 and 3.15. Equations 3.7 and 3.13 can then solved to obtain the value of B_{16}.

Now that extraction of ETM terms is mathematically shown to be obtained from ANSYS, the next step is to create the finite element model of the system and to outline the calculation of the strains and curvatures.

In order to model the system and applied forces as shown in Figure **3-5**, the base beam was constrained at the left end in all directions i.e. using clamped boundary conditions. Note that only the base beam has clamped boundary conditions. In the finite element model, this was achieved by setting u_x, u_y and u_z equal to zero at the left end of

the beam. The nodes at the tip of the beam were coupled in the x-direction. This is useful since the extensional axial force need not be distributed and applied to every node on the free tip end, but can be applied to just one node at the tip end of the beam. Figure **3-6** shows the boundary conditions and the applied extensional force.

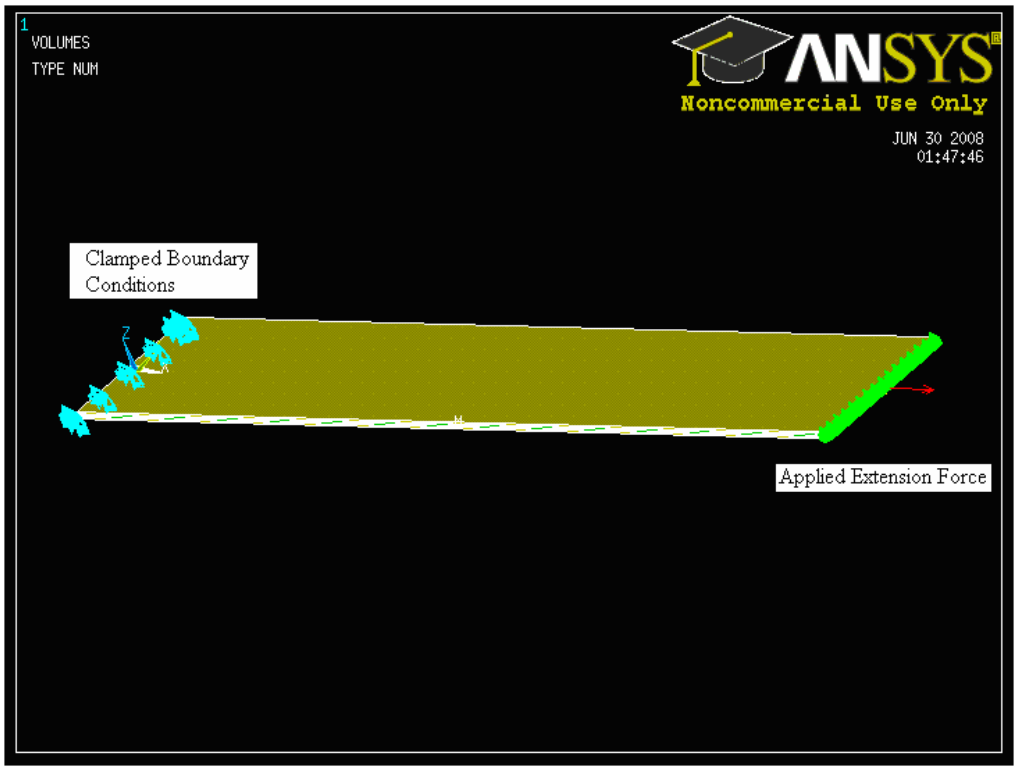

Figure **3-6**: Extension-Twist Analysis Boundary Conditions

Similarly, Figure **3-7** shows the application of a torque to the free end of the beam. Since SOLID 45 elements do not have rotational degrees of freedom, the torque was simulated by applying two opposite forces in the z direction at the end points of the beam as shown in Figure

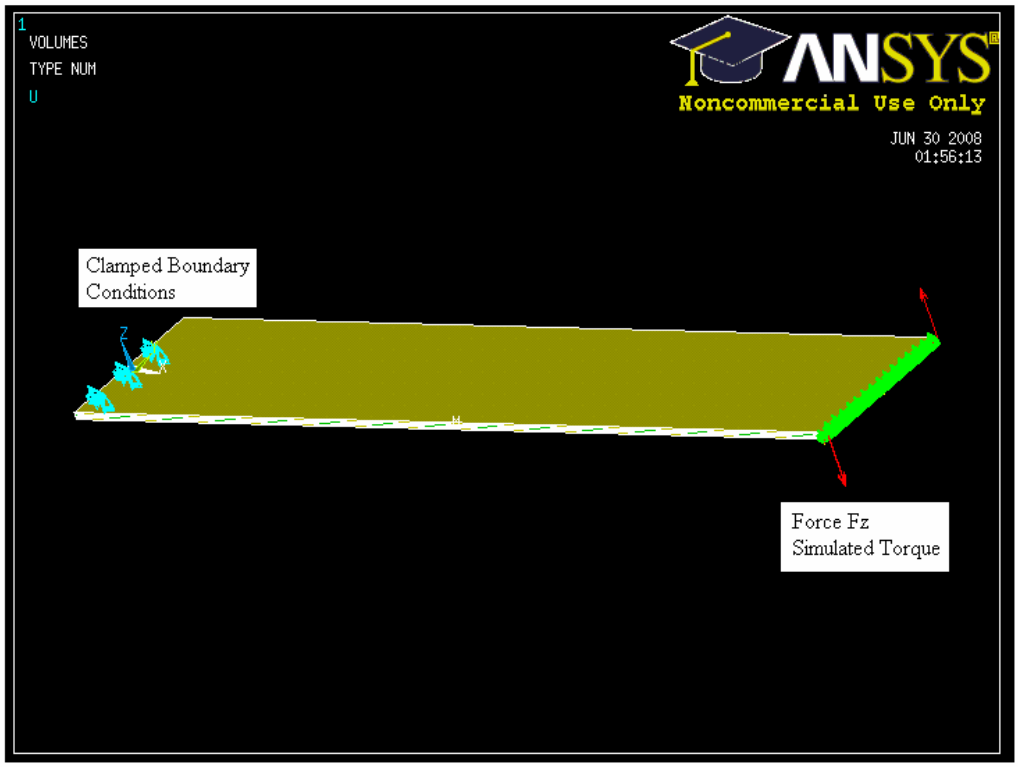

Figure **3-7**: Extension-Twist Analysis Application of Torque

Referring to Equations 3.9 and 3.15, the curvature twist term κ_{xy} needs to be obtained from the ANSYS solution. Figure **3-8** shows the coordinate system used in the analysis. The finite element model can output only strains (ε_{xx}, ε_{yy} and ε_{zz}) and displacements (u_x, u_y, and u_z). The following analysis describes the calculation of κ_{xy} from the output solution of ANSYS.

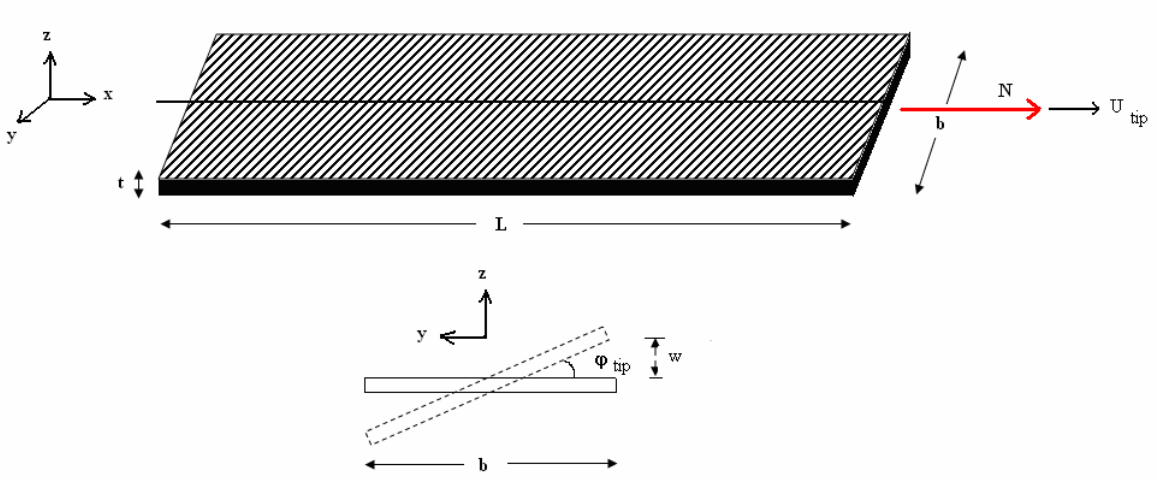

Figure **3-8**: Coordinate System used in ANSYS analysis

Referring to Figure **3-8**, φ_{tip} refers to the tip twist due to the coupling and u_{tip} refers to the tip axial displacement. The displacement in the *z* direction is denoted by *w*. Assume that the axial displacement and twist be expressed as follows in Equation **3.16** and Equation **3.17** respectively**:**

$$u_x = \left(\frac{x}{L}\right) u_{tip} \qquad \text{(Eq. } \mathbf{3.16}\text{)}$$

$$\phi = \left(\frac{x}{L}\right) \phi_{tip} \qquad \text{(Eq. } \mathbf{3.17}\text{)}$$

The displacement *w* is assumed as shown in Equation **3.18**.

$$w(x, y) = \left(\frac{x}{L}\right) \phi_{tip} y \qquad \text{(Eq. } \mathbf{3.18}\text{)}$$

Knowing the definition of ε_{xx} and κ_{xy} as a function of *w*, the following expressions are given in Equation **3.19** and Equation **3.20** :

$$\varepsilon_{xx} = \frac{\partial u}{\partial x} = \frac{u_{tip}}{L} \Rightarrow \quad u_{tip} = L\varepsilon_{xx} \qquad \text{(Eq. } \mathbf{3.19}\text{)}$$

$$\kappa_{xy} = 2\frac{\partial^2 w}{\partial x \partial y} = \frac{2\phi_{tip}}{L} \qquad \text{(Eq. } \mathbf{3.20}\text{)}$$

Equations 3.19 and 3.20 show the expressions for calculation of ε_{xx} and κ_{xy} from the outputs (ε_x and φ_{tip}) obtained from the ANSYS model. Recall the following Equations 3.9 and Equation 3.15.

$$N_{xx} = A_{11}\varepsilon_{xx} - D_{66}K_1 \qquad \text{(Eq. } \mathbf{3.21}\text{)}$$

$$M_{xy} = D_{66}\kappa_{xy} - A_{11}K_2 \qquad \text{(Eq. } \mathbf{3.22}\text{)}$$

In both Equations 3.9 and 3.15, the extraction ε_{xx} and κ_{xy} is shown and can be obtained through ANSYS. The applied axial force N_{xx} and applied torque M_{xy} are known quantities. The mathematics can be applied to the system in the coupled as well as the coupled state. Thus the only variables are the A_{11}, B_{16} and D_{66} terms which can be calculated by solution of the equations. Therefore in ANSYS it can be clearly seen that the A_{11}, B_{16} and D_{66} terms can be obtained for the coupled and decoupled states respectively. The ETM value as shown in Equation **3.23** can be hence calculated.

$$\text{Extension - Twist Metric} \quad (\text{ETM}) \quad = \quad \frac{\left|B_{16}^{2ply} - B_{16}^{4ply}\right|\left(A_{11}^{2ply} + A_{11}^{4ply}\right)\left(D_{66}^{2ply} + D_{66}^{4ply}\right)}{\left|A_{11}^{2ply} - A_{11}^{4ply}\right|\left|D_{66}^{2ply} - D_{66}^{4ply}\right|} \qquad \text{(Eq. } \mathbf{3.23}\text{)}$$

3.3.2 Extraction of Terms in the BTM

The BTM expression is shown in Equation **3.2**. On application of a bending moment only to the free end of the beam, the Force Resultant Matrix reduces to Equation **3.24** Refer to Appendix **A** for definition and derivation of terms.

$$\begin{Bmatrix} M_{xx} \\ M_{xy} \end{Bmatrix} = \begin{bmatrix} D_{11} & D_{16} \\ D_{16} & D_{66} \end{bmatrix} \begin{Bmatrix} \kappa_{xx} \\ \kappa_{xy} \end{Bmatrix} \qquad \text{(Eqn. 3.24)}$$

Figure **3-9** shows the moments and curvatures that are used in Equation **3.7**. $\mathbf{M_{xx}}$ is the moment about the y axis. $\mathbf{M_{xy}}$ is the applied torque. $\boldsymbol{\kappa_{xx}}$ and $\boldsymbol{\kappa_{xy}}$ refer to the bending curvature and twist curvature respectively.

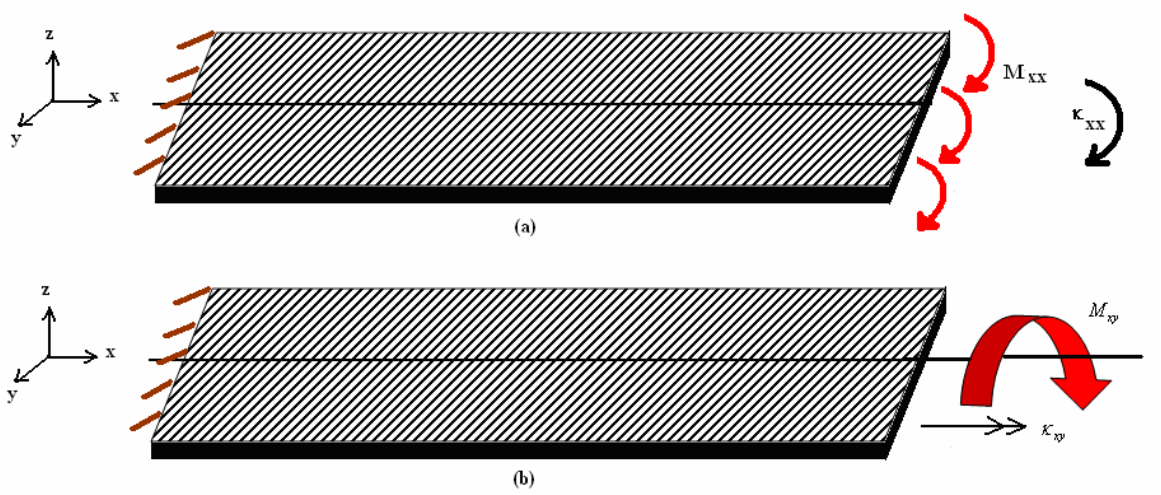

Figure **3-9**: Beam Applied Moments

As seen in Figure **3-9 (a)**, if only a known moment M_{xx}, and no torque (M_{xy}), is applied to the beam, Equation **3.22** reduces to Equation **3.25** .

$$\begin{Bmatrix} M_{xx} \\ 0 \end{Bmatrix} = \begin{bmatrix} D_{11} & D_{16} \\ D_{16} & D_{66} \end{bmatrix} \begin{Bmatrix} \kappa_{xx} \\ \kappa_{xy} \end{Bmatrix} \qquad \text{(Eqn. } \mathbf{3.25}\text{)}$$

Since M_{xx} is a known value, κ_{xx} and κ_{xy} can be obtained from the ANSYS output solution. Thus Equation **3.23** can be written as shown Equation **3.26** and Equation **3.27** :

$$M_{xx} = D_{11}\kappa_{xx} + D_{16}\kappa_{xy} \qquad \text{(Eq. } \mathbf{3.26}\text{)}$$

$$0 = D_{16}\kappa_{xx} + D_{66}\kappa_{xy} \qquad \text{(Eq. } \mathbf{3.27}\text{)}$$

Solving Equation 3.27 gives Equation **3.28**. Substituting Equation 3.28 into Equation 3.26 gives Equation **3.29.**

$$D_{16} = -\frac{D_{66}\kappa_{xy}}{\kappa_{xx}} \qquad \text{(Eq. } \mathbf{3.28}\text{)}$$

$$M_{xx} = D_{11}\kappa_{x} - D_{66}\frac{\kappa_{xy}^2}{\kappa_{xx}} \qquad \text{(Eq. } \mathbf{3.29}\text{)}$$

In Equation 3.29, assume the following

$$\frac{\kappa_{xy}^2}{\kappa_{xx}} = K_3$$

Substituting the value of K_3 in Equation 3.29 gives Equation **3.30**.

$$M_{xx} = D_{11}\kappa_{xx} - D_{66}K_3 \qquad \text{(Eq. } \mathbf{3.30}\text{)}$$

In Equation 3.30, M_{xx}, κ_{xx} and K_3 are known quantities that can be obtained from the ANSYS solution. Thus in this equation, D_{11} and D_{66} are the variables.

In the same beam, if only a known external torque M_{xy} is applied as shown in Figure **3-9 (b)**, in absence of an axial force Equation **3.24** reduces to Equation **3.31** .

$$\begin{Bmatrix} 0 \\ M_{xy} \end{Bmatrix} = \begin{bmatrix} D_{11} & D_{16} \\ D_{16} & D_{66} \end{bmatrix} \begin{Bmatrix} \kappa_{xx} \\ \kappa_{xy} \end{Bmatrix} \qquad \text{(Eqn. } \mathbf{3.31}\text{)}$$

By imposing a known external torque M_{xy} on the beam, another set of values of κ_{xx} and κ_{xy} can be obtained from the ANSYS output. Thus Equation **3.31** can be written as shown in Equation **3.32** and Equation **3.33** :

$$0 = D_{11}\kappa_{xx} + D_{16}\kappa_{xy} \qquad \text{(Eq. } \mathbf{3.32}\text{)}$$

$$M_{xy} = D_{16}\kappa_{xx} + D_{66}\kappa_{xy} \qquad \text{(Eq. } \mathbf{3.33}\text{)}$$

Solving Equation 3.32 gives Equation **3.34**. Substituting Equation 3.34 in Equation 3.33 gives Equation **3.35**.

$$D_{16} = -\frac{D_{11}\kappa_{xx}}{\kappa_{xy}} \qquad \text{(Eq. } \mathbf{3.34}\text{)}$$

$$M_{xy} = -\frac{D_{11}\kappa^2{}_{xx}}{\kappa_{xy}} + D_{66}\kappa_{xy} \qquad \text{(Eq. } \mathbf{3.35}\text{)}$$

In Equation 3.35, assume the following:

$$\frac{\kappa_{xx}^2}{\kappa_{xy}} = K_4$$

Substituting the value of K_4 in Equation 3.35 gives Equation **3.36**.

$$M_{xy} = D_{66}\kappa_{xy} - D_{11}K_4 \qquad \text{(Eq. } \mathbf{3.36}\text{)}$$

In Equation 3.36, M_{xy}, K_4 and κ_{xy} are known quantities obtained from the ANSYS solution. Note that the values of κ_{xy} and κ_{xx} obtained in Equations 3.30 and 3.36 are different since 3.30 was obtained under application of a bending moment only and 3.36 was obtained under application of an applied torque only.

Observation of Equations 3.30 and 3.36 indicate that they are two equations in two variables (unknowns) i.e. D_{11} and $D_{66.}$ All other terms areknown. Thus, the values of D_{11} and D_{66} can be obtained by solving Equations 3.30 and 3.36. Equations 3.28 and 3.34 can be solved to obtain D_{16}.

Since the extraction of required parameters in the BTM is shown, the next step is to develop the finite element model of the system and outline the calculation of the curvatures in Equations 3.30 and 3.36.

In order to model the system and applied moments as shown in Figure **3-9**, the beam was constrained on the left in all directions i.e. clamped boundary conditions. In the finite element model, this was achieved by setting u_x, u_y and u_z equal to zero at the left end of the beam. Figure **3-10** shows the boundary conditions and the applied bending force. The bending moment was simulated by applying a force $-F_z$ at the tip of the beam.Another alternative would be to apply a $+F_x$ and a $-F_x$ to the to the top and bottom of the base beam respectively to represent the bending moment M_{xx}. Figure **3-11** shows the application of a torque to the free end of the beam. The torque was simulated by applying two opposite forces in the *z* direction at the end points of the beam. This is shown in Figure **3-11**.

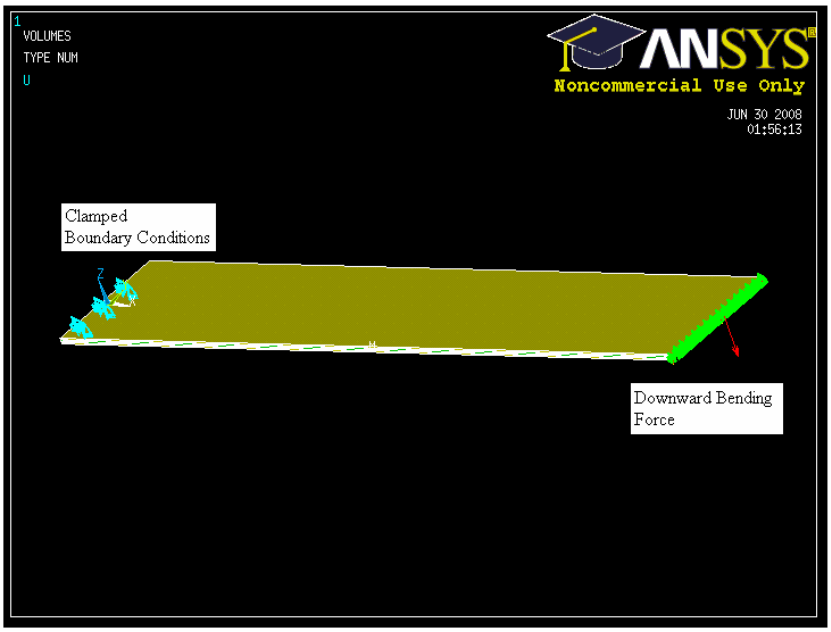

Figure **3-10**: Bending-Twist Analysis Boundary Conditions

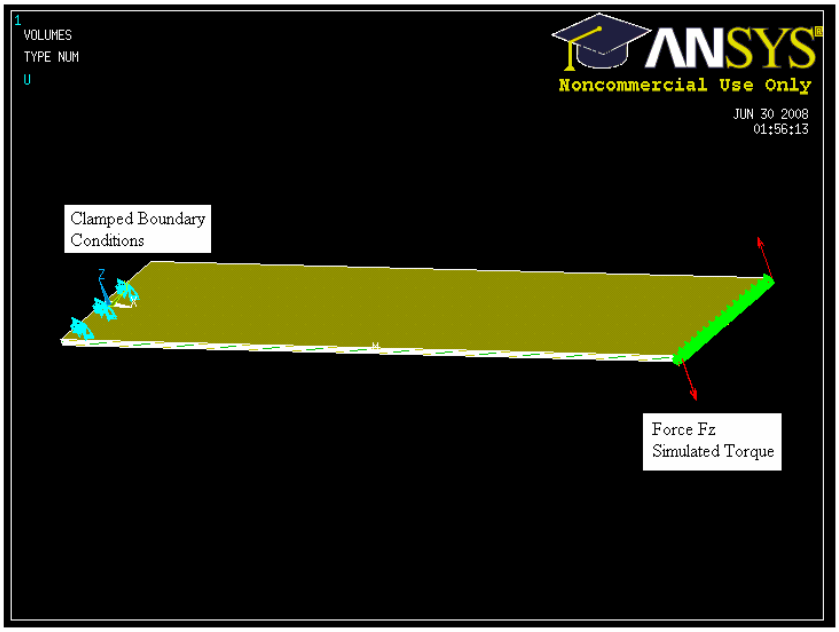

Figure **3-11**: Bending-Twist Analysis Application of Torque

From Equations 3.30 and 3.36, the curvature terms κ_{xx} and κ_{xy} need to be obtained. Figure **3-12** shows the coordinate system used in the analysis. The finite element model can output only strains (ε_x, ε_y and ε_z) and displacements (u_x, u_y, and u_z). The following analysis describes the calculation of κ_{xx} and κ_{xy} from the output solution of ANSYS.

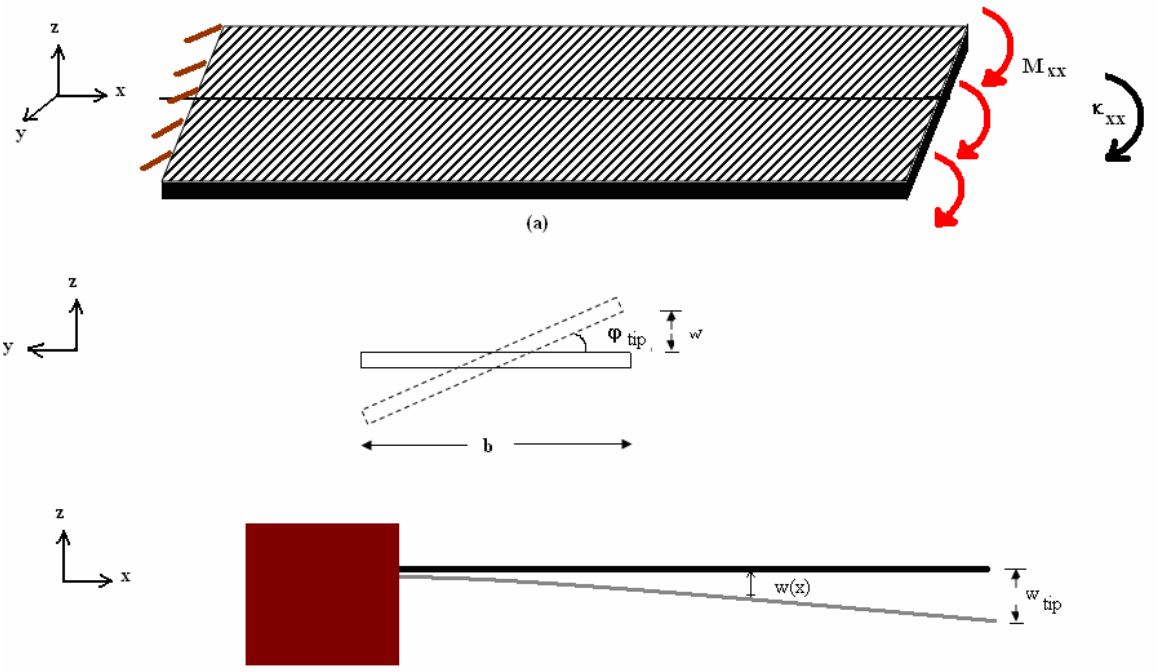

Figure **3-12**: BTM coordinate system used in ANSYS model

The displacement in the z direction is denoted as w. The twist at the tip is denoted by φ_{twist}. Note the length of the beam is *L* and width is *b*. The vertical displacement w is assumed as shown in Equation **3.37** :

$$w(x,y) = a\left(\frac{x}{L}\right)^2 + \phi_{tip}\left(\frac{x}{L}\right)y \qquad \text{(Eq. 3.37)}$$

where *a* is a constant that is dependent on the stiffness and applied bending moment. From the definition of κ_{xy} and κ_{xx} as given in Equation **3.38** and Equation **3.39**.

$$\kappa_{xy} = 2\frac{\partial^2 w}{\partial x \partial y} \quad \text{(Eq. } \mathbf{3.38}\text{)}$$

$$\kappa_{xx} = \frac{\partial^2 w}{\partial x^2} \quad \text{(Eq. } \mathbf{3.39}\text{)}$$

Differentiating the value of *w* in Equation 3.37 according to Equations 3.38 and 3.39 gives Equation **3.40** and Equation **3.41**.

$$\kappa_{xy} = 2\frac{\phi_{tip}}{L} \quad \text{(Eq. } \mathbf{3.40}\text{)}$$

$$\kappa_{xx} = \frac{2a}{L^2} \quad \text{(Eq. } \mathbf{3.41}\text{)}$$

Equation 3.40 enables the calculation of κ_{xy} from the tip twist output obtained from ANSYS. In order to calculate κ_{xx}, the vertical displacements of the centerline along are plotted as a function of *x*. The graph of *w(x)* verses *x* is a quadratic curve. Fitting an equation to this curve gives an expression for *w(x)*. This expression can be analytically differentiated twice to obtain the value of $\frac{\partial^2 w}{\partial x^2}$.

Thus, the values of κ_{xx} and κ_{xy} can be obtained from the ANSYS model. Recalling Equations 3.30 and 3.36:

$$M_{xx} = D_{11}\kappa_{xx} - D_{66}K_3 \quad \text{(Eq. } \mathbf{3.42}\text{)}$$

$$M_{xy} = D_{66}\kappa_{xy} - D_{11}K_4 \quad \text{(Eq. } \mathbf{3.43}\text{)}$$

In both the above equations, the extraction κ_{xx} and κ_{xy} is shown and can be obtained through ANSYS. The applied bending moment M_{xx} and applied torque M_{xy} are known quantities. The mathematics can be applied to the system in the coupled as well as the coupled state. Thus the only variables are the D_{11}, D_{16} and D_{66} terms which can be calculated by solution of the equations. Therefore in ANSYS it can be clearly seen that the D_{11}, D_{16} and D_{66} terms can be obtained for the coupled and decoupled states respectively. The BTM value as shown in Equation **3.44** can thus be calculated from ANSYS.

$$\text{Bending} - \text{Twist Metric } (BTM) = \frac{\left|D_{16}^{2\,ply} - D_{16}^{4\,ply}\right|\left(D_{11}^{2\,ply} + D_{11}^{4\,ply}\right)\left(D_{66}^{2\,ply} + D_{66}^{4\,ply}\right)}{\left|D_{11}^{2\,ply} - D_{11}^{4\,ply}\right|\left|D_{66}^{2\,ply} - D_{66}^{4\,ply}\right|} \qquad \text{(Eqn. 3.44)}$$

3.3.3 Schematics and Screenshots of ANSYS Model

Figure **3-13** shows a screenshot of the multi-layered beam modeled in ANSYS. SOLID 45 elements were used to model the system. Figure **3-14** shows a close-up view of the different layers in the beam. Figure **3-15** shows the meshed model in ANSYS. Figure **3-16** shows a close-up of the meshed layers in the model. Note that the inner and outer plies have 3 elements through the thickness. The polymer layer also has 3 elements through the thickness. Table **3-5** summarizes the different meshing parameters used in the ANSYS model

Figure **3-13**: Screenshots of Beam modeled in ANSYS

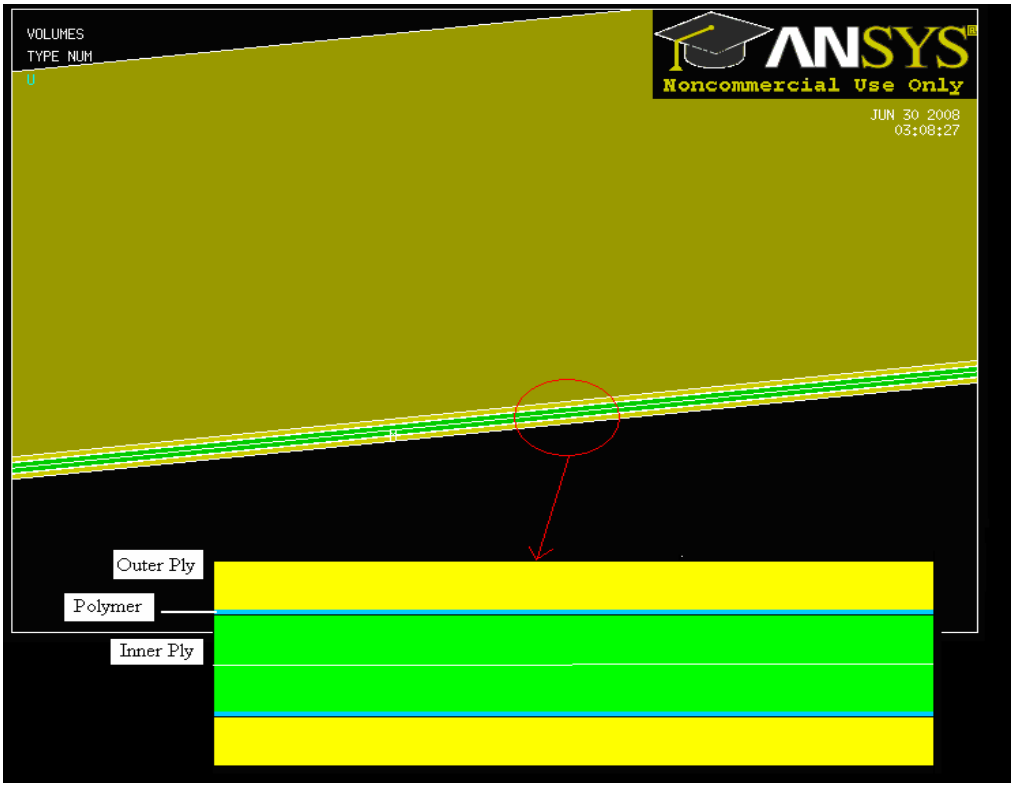

Figure **3-14**: Close-up of Multi-layered Beam modeled in ANSYS

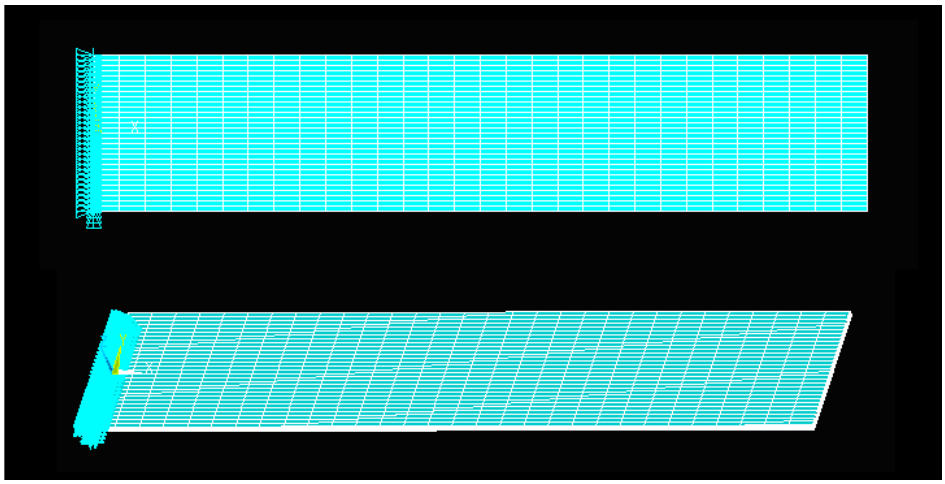

Figure **3-15**: Multi-layered Beam Mesh Model

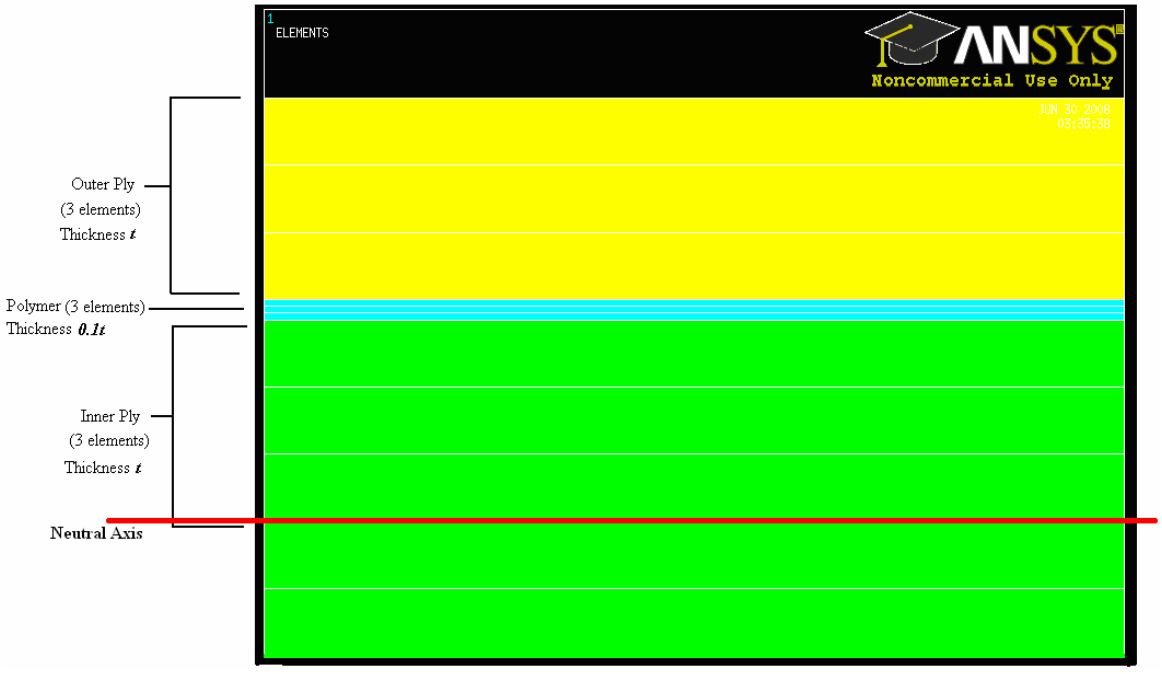

Figure **3-16**: Close-up of Meshed Layers in ANSYS Model

Table **3-5**: Meshing Parameters in ANSYS Model

1. Parameter	**2. Value**
3. Mesh Size	4. 30 elements along length L 5. 30 elements along width b 6. 18 elements through total thickness
7. Mesh Shape	8. Quadrilateral
9. Number of Elements along Length L	10. 30
11. Number of Elements along Width b	12. 30
13. Number of Elements along Each Layer Thickness t	14. 3
15. Total Number of Elements	16. 16200
17. Total Number of Nodes	18. 178746

3.3.4 Results Convergence Tests

In order to ensure the validity of the model in solving the equations to depict the shear in the polymer layer to act as a decoupling medium, a convergent study is done on two parameters in the ANSYS finite element model. These were the thickness of the

polymer layer and the number of elements through the thickness of the polymer layer. Initially the thickness of the polymer layer is set as 0.5 times the thickness of the plies. The stiffness coefficients and hence the ETM and BTM are obtained through the analysis mentioned in Section **3.3.1**.and **3.3.2**. The thickness is then reduced in increments of 0.1 until a convergence in the solution (i.e. stiffness coefficients) was obtained. The results of this convergent study are shown in Chapter **4.**

The second convergence study is done on the number of elements through the thickness of the polymer layer. When the polymer layer's shear modulus is reduced by three orders of magnitude, the shear in the polymer layer decouples the inner plies from the outer plies. In order to capture this effect, more elements need to be modeled though the thickness of polymer layer. Thus initially the solution was obtained with just one element though the thickness. Next, the number of elements was increased to two, three and four respectively. Increasing the number of elements beyond four leads to excess computational requirements, which are not available at this time of research. The results of this convergence study are also shown in Chapter **4**.

Chapter 4

RESULTS AND DISCUSSIONS

The composite multi-layered beam was modeled in Matlab as described in Chapter **3**. The computer code was run for various different orientations of plies in the laminate. Using a 2-ply system and a 4-ply system, the values of the metrics were computed. These values are shown graphically in the following sections. Also the individual values of the terms in the metrics are shown graphically.

The values of the metric obtained through Matlab analysis is then verified through ANSYS by comparing the values of terms extracted from ANSYS to those displayed by the Matlab program. This preliminary ANSYS simulation does not incorporate the polymer layers in the model. After the desired laminate with the highest metric value is chosen through the Matlab analysis, the system is then modeled in ANSYS with the polymer layers and the effect of the polymer layers is analyzed. The effect of the polymer layer in decoupling the system is identified. The results are presented for both the Extension-Twist Metric (ETM) and the Bending-Twist Metric (BTM).

4.1 Extension Twist Metric (ETM)

4.1.1 Matlab Analysis

Material properties and dimensions of the multi-layered beam are given in Table **3-1** and Table **3-2** respectively. For a composite laminate to have extension-twist coupling, the lay-up needs to be antisymmetric about the mid-plane. Thus the multi-beam lay-up was setup as *[-α / θ /-θ / α]*. The outer plies are denoted as α and the inner plies are denoted as θ. The ETM is calculated for different values of the inner and outer ply

orientation angle in the laminate. In order to calculate the coefficients of the ETM, the analysis was run first using the perfectly decoupled and then the perfectly coupled state. Details of this method can be found in Chapter 3. The outer ply angles were varied from -90° to + 90° and the inner ply angles were varied from 0° to 90°. This ensured that all possible combinations of ply orientations were possible and also ensured that an antisymmetric lay-up was obtained. The ply angles were varied in increments of 15 degrees. Figure **4-1** shows the variation of the ETM for different values of inner and outer ply angles. Note that the Matlab model does not include the effects of the polymer layer.

Each point on the graph in Figure **4-1** represents a particular laminate with a particular *[-α / θ /-θ / α]* lay-up. The x-axis corresponds to the variation of the outer ply angle. Each color represents the respective inner ply angle. The y axis corresponds to the value of the ETM for each laminate.

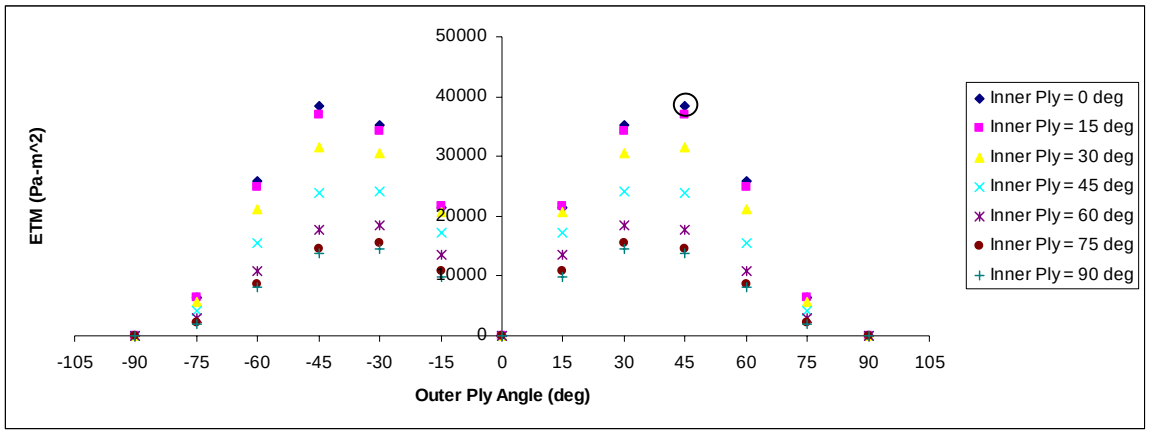

Figure **4-1**: ETM Laminate Analysis in Matlab

Thus noting that the dot circled in Figure **4-1** has the highest ETM value, according to the legend on the right, it corresponds to an inner ply angle of 0°. Following this point along the horizontal axis indicates that it corresponds to an outer ply angle of 45°. The graph is symmetric about the x-axis, thus choosing an outer ply angle of -45° is also theoretically the correct choice. Since each point on this graph represents a laminate, the circled point corresponds to the **[-45/0/0/45] °** laminate. Thus the ETM predicts that this laminate will have the highest change in coupling but at the same time ensuring that the extensional and torsional stiffness's were not compromised.

$$\text{Extension - Twist Metric} \quad (\text{ETM}) \quad = \quad \frac{\left|B_{16}^{2ply} - B_{16}^{4ply}\right|\left(A_{11}^{2ply} + A_{11}^{4ply}\right)\left(D_{66}^{2ply} + D_{66}^{4ply}\right)}{\left|A_{11}^{2ply} - A_{11}^{4ply}\right|\left|D_{66}^{2ply} - D_{66}^{4ply}\right|} \qquad \text{(Eqn. 4.1)}$$

Equation **4.1** shows the different terms in the ETM. In order to analyze the choice of laminate chosen by the ETM, each term in the ETM is plotted as a function of inner and outer ply angles. This is done to analyze the choice of laminate ply orientation by the ETM. i.e. why does the ETM tend to choose he [-45/0/0/45] laminate? Similarly, each point on the following graphs represents a particular lay-up.

Figure **4-2** shows the variation of the change in B_{16}, i.e. the change in the coupling parameter between the coupled and the decoupled states. It is observed that the change in B_{16} is independent of the given inner ply angle. This implies that the change in coupling is dependent on the choice of the outer ply angle. As can be seen in Figure **4-2**, choosing an outer ply angle of 45° gives a high value of change in coupling which is desired. The greatest change in B16 is when the outer ply angle is 30°.

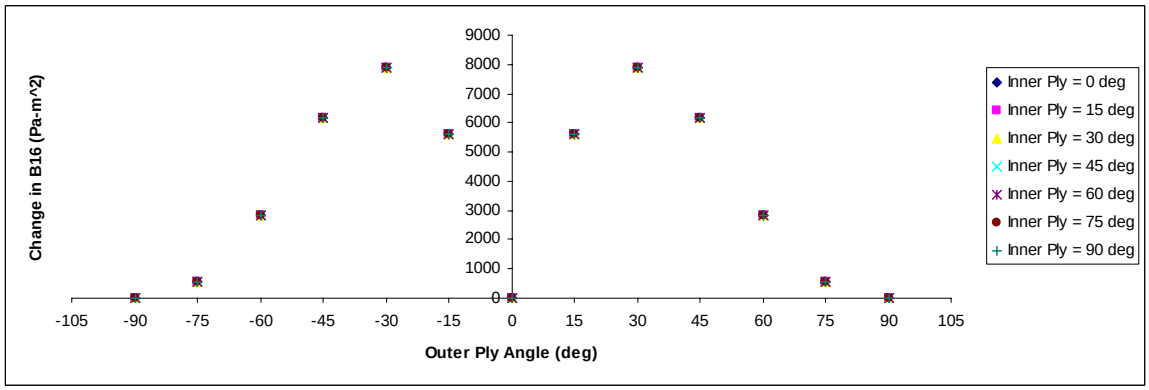

Figure **4-2**: Variation of Change in Coupling term in ETM

Referring to Equation **4.1**, the term in the denominator is the change in A_{11}, i.e. the change in extensional stiffness between the coupled and decoupled states. On application of an extensional load, the extensional stiffness of the structure should not

drastically reduce due to the decoupling of the system. Thus this value of change in A_{11} should be low. Figure **4-3** shows the variation of change in extensional stiffness (A_{11}) for different orientations of inner and outer ply angles. From Figure **4-3**, it is clear that the change in A_{11} is not sensitive to inner ply angle. The ETM indicated an outer ply angle of 45° as seen in Figure **4-1**. From Figure **4-3**, it can be seen that choosing a 45° outer ply angle gives a moderately low value for change in extensional stiffness. This value is also symmetric about the y axis.

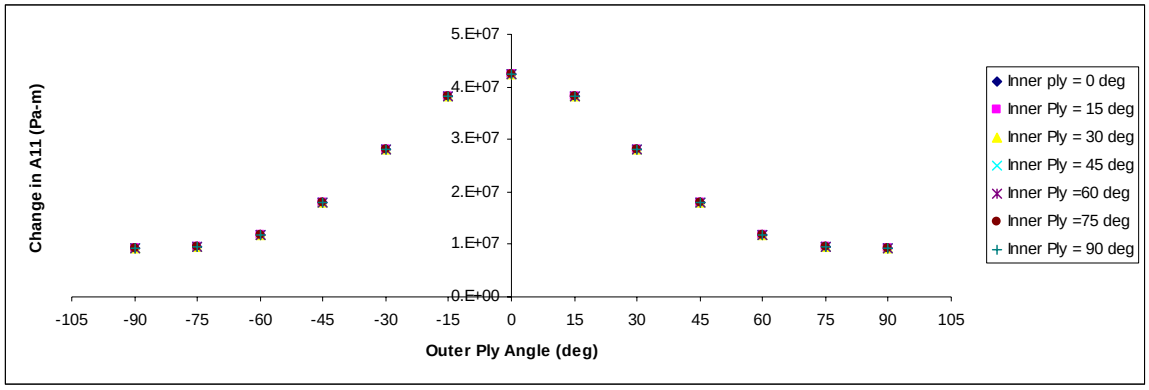

Figure **4-3**: Variation of Change in Extensional Stiffness term in ETM

The second term in the denominator of Equation **4.1** is the change in torsional stiffness (D_{66}) between the coupled and decoupled states. As before, the torsional stiffness of the system should not be drastically changed due to the decoupling of the inner plies from the outer plies. Figure **4-4** shows the change in torsional stiffness with different laminate orientations. It can be seen that the difference in torisonal stiffness is not sensitive to choice of inner ply angle, but choosing an outer ply angle of 45° gives a comparatively high value for this change in torsional stiffness. Symmetry about the y axis is again observed.

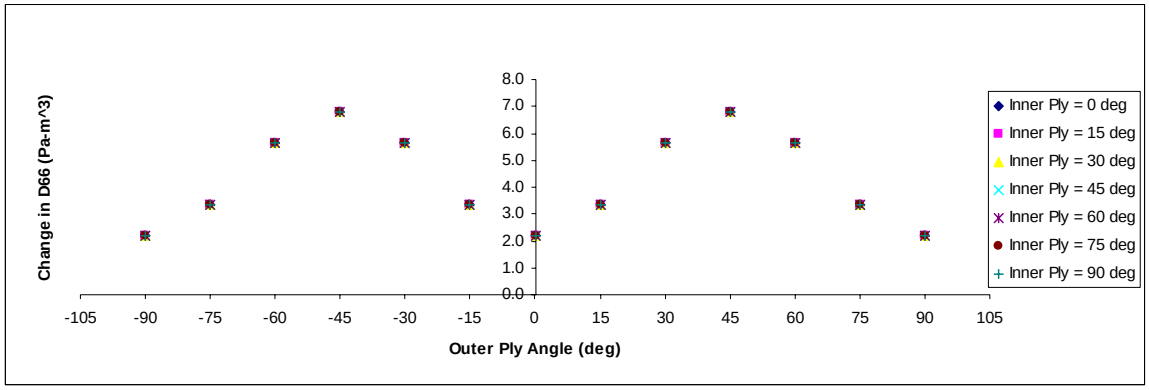

Figure **4-4**: Variation of Change in Torsional Stiffness term in ETM

The numerator of Equation **4.1** also contains the mean extensional and torisonal stiffness of the 2-ply and 4-ply configurations. It is desired that the value of these terms be high as required of a load-bearing structure. Figure **4-5** shows the variation in the mean extensional stiffness in the coupled and decoupled states for different laminate configurations. The mean extensional stiffness is dependent significantly on the choice of inner ply angle orientation and also on outer ply angle orientation. It can be seen in Figure **4-5** that choosing an inner ply angle of 0° (solid blue diamonds) at an outer ply angle of 45° produces a high value for the mean extensional stiffness.

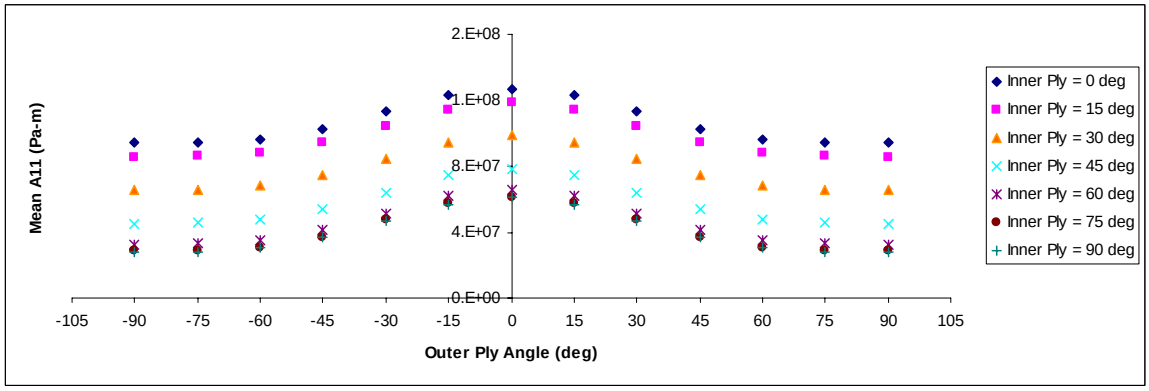

Figure **4-5**: Variation in Mean Extensional Stiffness terms in ETM

The mean torsional stiffness in the coupled and decoupled states is plotted in Figure **4-6** for various laminate ply orientations. It can be observed that this term is moderately sensitive to the inner ply angle and relatively more sensitive to the outer ply angle. The value is again symmetric about the x-axis. From Figure **4-6**, for an outer ply angle of 45° , the highest mean torsional stiffness is observed when the inner plies are also at 45°. However, an inner ply angle of 0° (which leads to high mean extensional stiffness and higher ETM) does not result in a significant decrease in mean torsional stiffness.

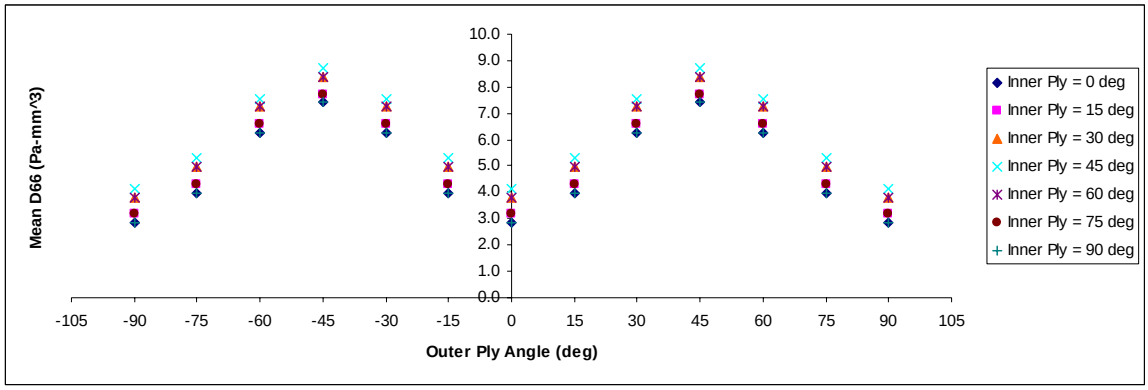

Figure **4-6**: Variation in Mean Torsional Stiffness terms in ETM

Thus the ETM's choice of the **[-45/0/0/45] °** laminate is justified since the choice of the outer and inner ply angles correspond to the desired trends in the values of the terms in Equation **4.1**. It can be observed that the change in coupling (ΔB_{16}), change in extensional stiffness (ΔA_{11}) and change in torsional stiffness (ΔD_{66}) are independent of the inner ply angle orientation. The mean extensional stiffness and mean bending stiffness terms are comparatively more sensitive to inner ply orientation. But at the same time, they are highly sensitive to outer ply orientation as well.

4.1.2 ANSYS Analysis

In order to validate the numerical finite element analysis solution of terms in the ETM from the ANSYS solution, the multi-layer beam is first modeled in ANSYS without the inclusion of the polymer layer. Refer to Chapter **3** for details on extraction of ETM terms from ANSYS. Since the Matlab analysis showed that the ETM predicts a maximum value for the [-45/0/0/45] laminate, the first simulation run in ANSYS was keeping the inner ply angle as 0° and varying the outer ply angle from -90° to 90°.

In order to extract the parameters required to compute the ETM, two test forces were applied to the beam model in ANSYS. First, an extensional force F_x = 1 N was applied to the multi-layer beam as shown in Chapter **3**. The tip displacement and strain outputs were obtained. Second, a torque of M_{xy} = 1 N-m was applied and the displacement outputs were obtained. These were used to calculate the A_{11}, B_{16}, and D_{66} terms in Equation **4.1**. Note that the ANSYS analysis was first done for inner ply angle of 0° and varying the outer ply angle thus modeling the ideal 4 ply and 2 ply cases.

Thus using the values of A_{11}, B_{16}, and D_{66} terms obtained from ANSYS, the ETM was calculated again. The results are shown in Figure **4-7.** It can be seen that values of the ETM obtained from ANSYS closely match those provided by Matlab for the ideal case. The data agrees with a 4.04% error.

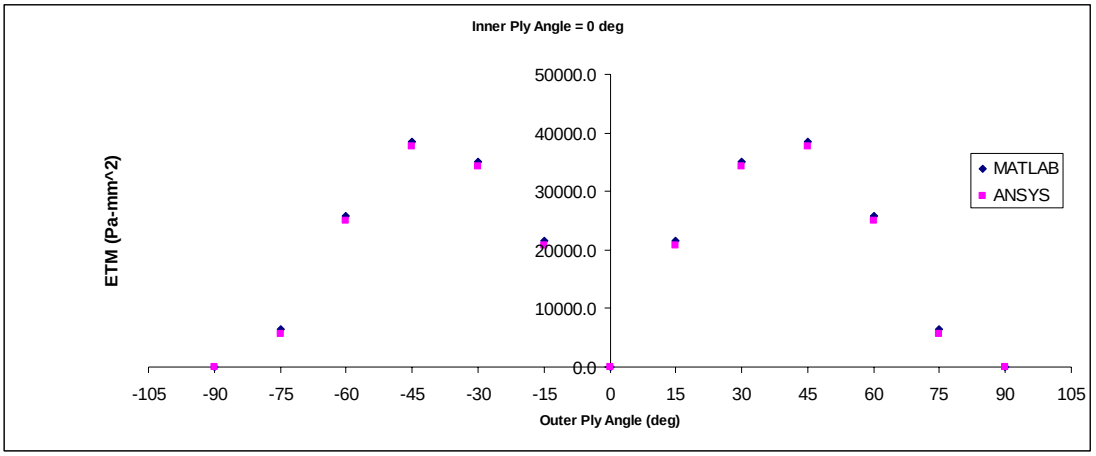

Figure **4-7**: Comparison of Matlab and ANSYS for the [-α/0/0/α] laminate

After validating the numerical solution of the terms in the ETM obtained through the ANSYS model, the polymer layers are then introduced in the ANSYS model. To simulate the "glassy" and "rubbery" polymer states respectively, the material properties were assigned to the polymer layer as given in Table **3-2**.

Since the Matlab model indicated the [-45/0/0/45] laminate produced the highest value of the ETM, this laminate orientation will be used to model the multi-layered beam with the polymer layers in ANSYS. The ply thickness is set at 0.5 mm. The presence of the polymer layer thickness affects the results of the analysis. Figure **4-8** shows the ETM with decreasing polymer layer thickness. It can be seen that in between 30% to 10% of the ply thickness, the ETM approaches the ideal solution. For thicker polymer layers, coupling between inner and outer plies cannot be achieved. From Figure **4-8**, it can be seen that the ETM value with the polymer layer at one-tenth the ply thickness approaches the ideal no bond assumption case, i.e. 0*t*. This value of polymer thickness (0.1 times the ply thickness) will be used in further analysis from this point onwards.

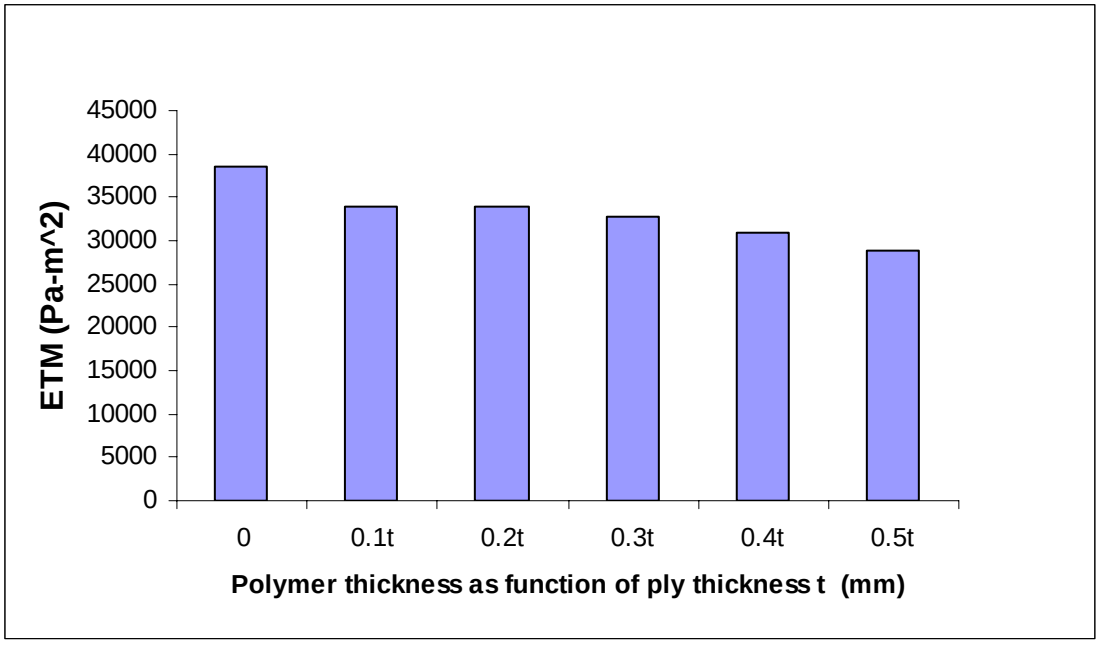

Figure **4-8**: ETM Value as a function of Polymer Thickness for [-45/0/0/45] Laminate

In order to accurately depict the shear effects of the polymer layer, the number of solid elements through the polymer layer thickness was increased from one to four elements. Although increasing the number of elements increases computation time, the goal is to obtain a convergent solution. From this, a convergence study is done which shows the variation of the ETM value with increasing the number of elements through the polymer thickness. Figure **4-9** shows the results of this grid independence or convergence study. From the figure, choosing 3 or 4 elements per layer gives a convergent result. In order to reduce computational requirements, 3 elements were used through the polymer layer thickness to model the shear effects of the polymer layer. Thus the analysis from this point onwards uses 3 elements through the thickness of each layer.

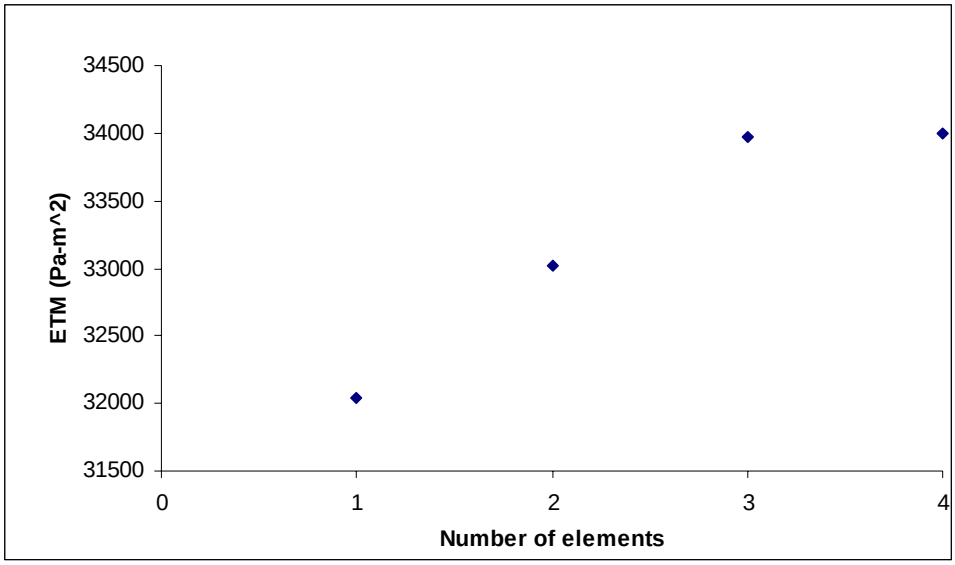

Figure **4-9**: Convergence Study of Varying Number of Elements through Polymer Layer Thickness for the [-45/0/0/45] Laminate.

Table **4-1** summarizes the modeling parameters used in the ETM ANSYS model with the polymer layers included. The definition and description of these terms can be found in Chapter **3.3**

Table **4-1**: Summary of ETM ANSYS Modeling Parameters

Parameter	**Value**
Element Type	SOLID 45
Thickness of Polymer Layer	0.05 mm
Mesh Type	Quadrilateral
Mesh Size of the polymer	30 elements along length 30 elements along width 3 elements through thickness
Boundary Conditions	• At x = 0, y , z : u_x, u_y, u_z = 0 (Clamped Boundary Conditions) • At x = 0.254, y, z : F_x (Axial Force at tip)
Outputs	• Displacements: u_x, u_y, u_z • Strain: ε_x

Figure **4-10** shows the comparison of ETM results between Matlab and ANSYS. As discussed in Chapter 3, in Matlab, a perfect bond assumption was made between the four plies and the Matlab results pertain to perfectly coupled and decoupled systems. In ANSYS the results approach the perfect bond assumption results as can be seen in Figure **4-10**. The blue bar represents the ETM value for the perfectly decoupled case (Matlab Analysis) and the magenta bar represents the ETM value calculated from the ANSYS model. The modulus of the polymer layer was reduced by three orders of magnitude so as to model the 'soft' polymer. The difference in the ETM between ANSYS and Matlab model is due to the effect of the finite thickness and stiffness of the polymer layer modeled in ANSYS. As expected, the shear effects of the polymer layer tend to decouple the system, but due to the polymer's finite thickness and stiffness, the inner two plies are never completely decoupled from the outer two plies.

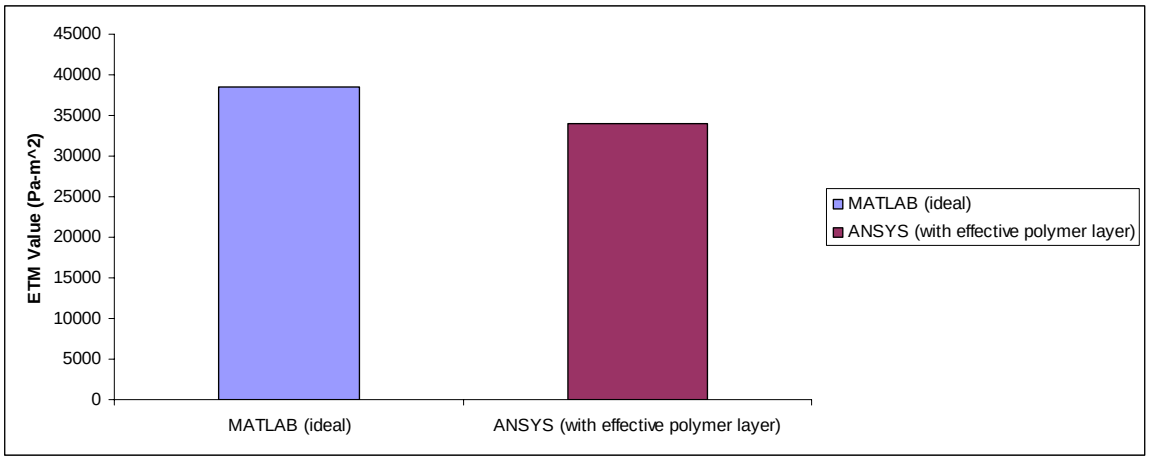

Figure **4-10**: Comparison of ETM between Matlab and ANYS model with polymer layers for the [-45/0/0/45] laminate

As the ETM is highly dependent on the coupling parameters, as the polymer went through its glass transition, the beam outer layers were decoupled. Hence Figure **4-11** shows the comparison in the coupling parameter B_{16} between the glassy and rubbery polymer states respectively. The blue bars represent the ideal Matlab state. Here the coupling parameter has a high value when the four plies are in the coupled state. But in the perfectly decoupled 2-ply state, since the inner two plies are 0°, no coupling exists and thus the B_{16} term goes to zero.

The pink bars represent the ANSYS model calculation of B_{16}. In the 4-ply case, the value of the coupling parameter is high when the polymer layer is stiff. But when the polymer layer is in the 'soft' state, since the inner plies are not completely decoupled from the outer plies, the influence of the outer plies affects the coupling parameter in the soft polymer state. This is evident from Figure **4-11**. When the polymer is soft, even though the inner plies are 0°, the influence of the outer plies does not make the last pink bar in the figure go to zero.

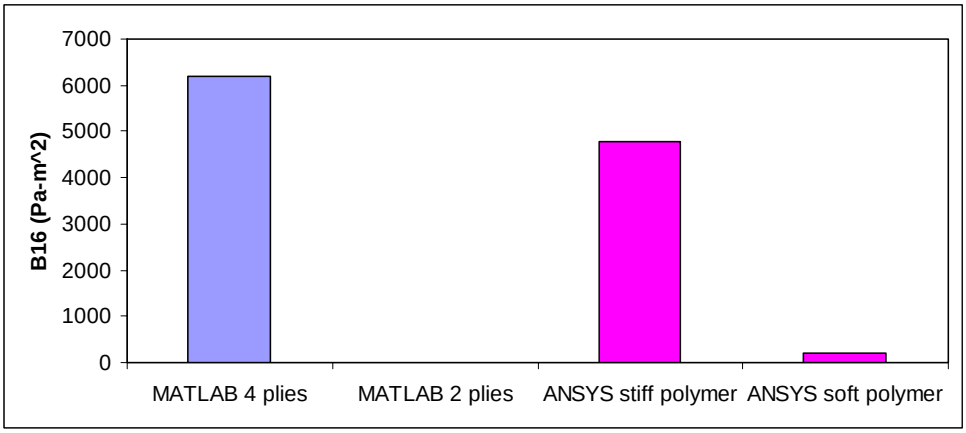

Figure **4-11**: Comparison of ANSYS and Matlab B_{16} results for [-45/0/0/45] laminate

4.2 Bending Twist Metric (BTM)

4.2.1 Matlab Analysis

Material properties and dimensions of the multi-layered beam are given in Table **3-1** and Table **3-2** respectively. For a composite laminate to exhibit bending-twist coupling, the ply lay-up needs to be symmetric about the mid-plane. Thus the multi-beam lay-up was setup as *[α / θ / θ / α]*. The outer plies are denoted as α and the inner plies are denoted as θ. The BTM is calculated for different values of the inner and outer ply orientation angle in the laminate. In order to calculate the coefficients of the BTM, the analysis was run first using the perfectly decoupled and then the perfectly coupled state. Details of this method can be found in Chapter **3**. The outer ply angles were varied from -90° to + 90° and the inner ply angles were varied from 0° to 90°. This ensured that all possible combinations of ply orientations were possible. The ply angles were varied in increments of 15 degrees. Figure **4-12** shows the variation of the BTM for different values of inner and outer ply angles. Note that the Matlab model does not include the effects of the polymer layer.

Similar to the ETM analysis, each point on the graph in Figure **4-12** represents a particular laminate with a *[α / θ / θ / α]* lay-up. The x-axis corresponds to the variation of the outer ply angle. Each color represents the respective inner ply angle. The y-axis corresponds to the value of the ETM for each laminate.

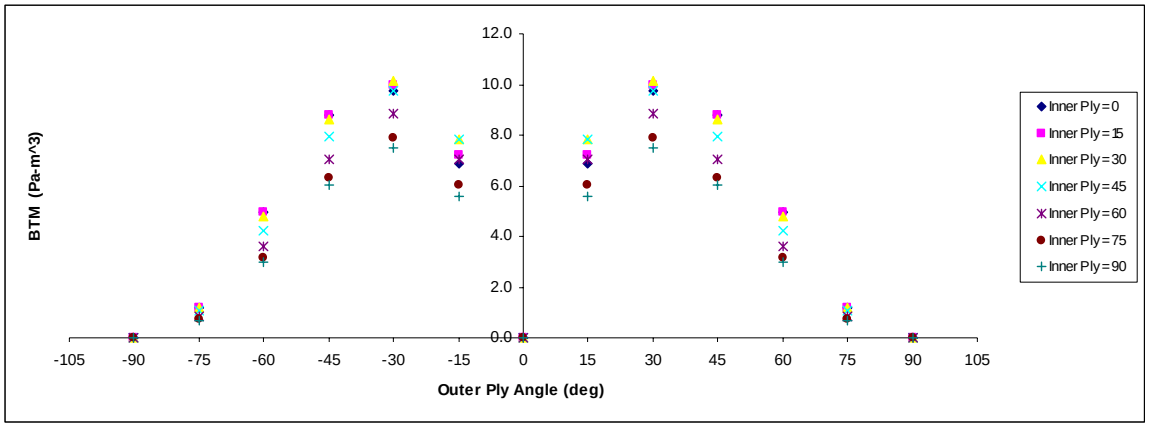

Figure **4-12**: BTM Laminate Analysis in Matlab

In Figure **4-12**, the point that has the highest BTM value, according to the legend on the right, it corresponds to an inner ply angle of 30°. Following this point along the horizontal axis indicates that it corresponds to an outer ply angle of 30°. The graph is symmetric about the x-axis, thus choosing an outer ply angle of -30° is also theoretically the correct choice. Since each point on this graph represents a laminate, the highest point corresponds to the **[30/30/30/30] °** laminate. Thus the BTM predicts that this laminate will have the highest change in coupling but at the same time ensuring that the bending and torsional stiffness's are not compromised.

$$\text{Bending} - \text{Twist Metric } (BTM) = \frac{\left|D_{16}^{2ply} - D_{16}^{4ply}\right|\left(D_{11}^{2ply} + D_{11}^{4ply}\right)\left(D_{66}^{2ply} + D_{66}^{4ply}\right)}{\left|D_{11}^{2ply} - D_{11}^{4ply}\right|\left|D_{66}^{2ply} - D_{66}^{4ply}\right|} \qquad \text{(Eqn. 4.2)}$$

Equation **4.2** shows the different terms in the BTM. In order to analyze the choice of laminate chosen by the BTM, each term in the BTM is plotted as a function of inner

and outer ply angles. This is done to analyze the choice of laminate ply orientation by the BTM. i.e. why does the BTM tend to choose he [30/30/30/30] laminate. Similarly each point on the following graphs represents a particular lay-up.

Figure **4-13** shows the variation of the change in D_{16}, i.e. the change in the coupling parameter between the coupled and the decoupled states. It is observed that the change in D_{16} is independent of the inner ply angle. This implies that the change in coupling is dependent on the choice of the outer ply angle. As can be seen in Figure **4-13**, choosing an outer ply angle of 30° gives the higher value of change in coupling which is desired. This outer ply angle is the same as that predicted by the BTM.

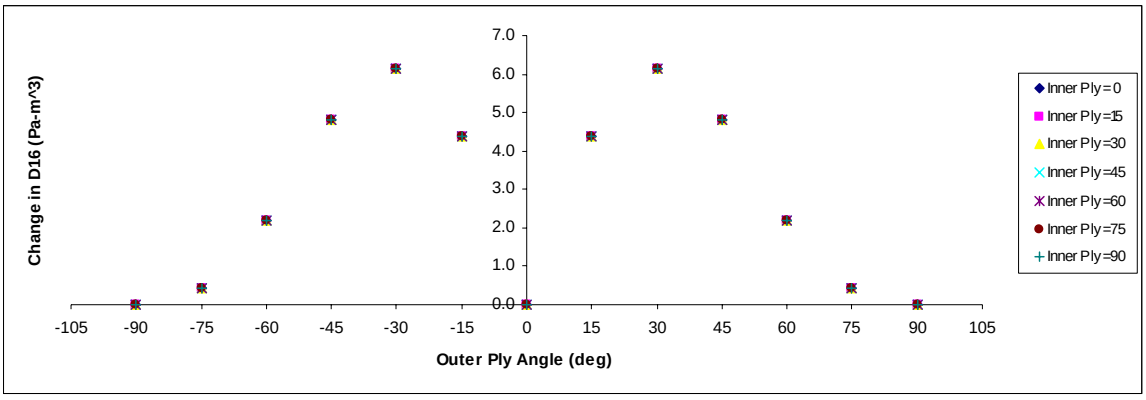

Figure **4-13**: Variation of Change in Coupling term in BTM

Referring to Equation **4.2**, the term in the denominator is the change in D_{11}, i.e. the change in bending stiffness between the coupled and decoupled states. On application of a bending moment, the bending stiffness of the structure should not drastically reduce due to the decoupling of the system. Thus this value of change in D_{11} should be low. Figure **4-14** shows the variation of change in bending stiffness (D_{11}) for different orientations of inner and outer ply angles. From Figure **4-14**, it is clear that the change in D_{11} is not sensitive to inner ply angle. The BTM indicated an outer ply angle of 30° as seen in Figure **4-12**. From Figure **4-14**, it can be seen that choosing a 30° outer ply angle gives a moderate value for change in bending stiffness.

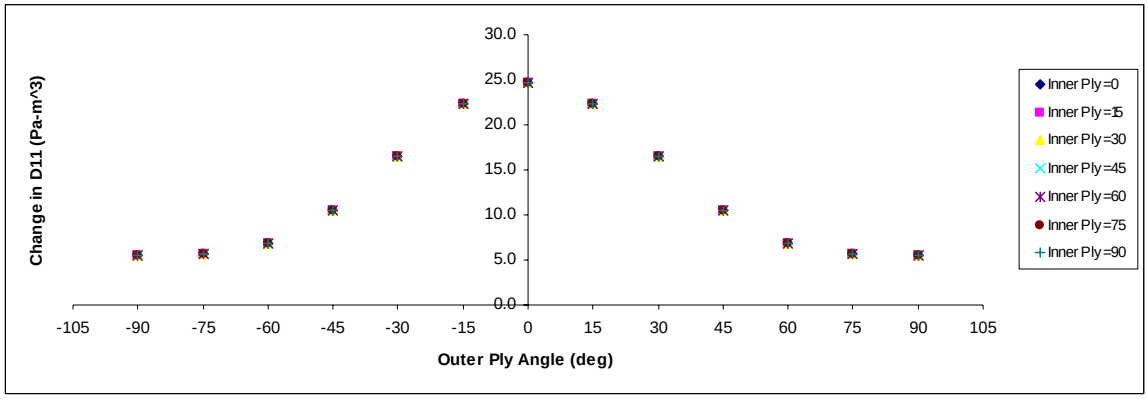

Figure **4-14**: Variation in Change of Bending Stiffness term in BTM

The second term in the denominator of Equation **4.2** is the change in torsional stiffness (D_{66}) ideally between the coupled and decoupled states. As before, the torsional stiffness of the system should not be drastically changed due to the decoupling of the inner plies from the outer plies. Figure **4-15** shows the change in torsional stiffness with different laminate orientations. It can be seen that the difference in torisonal stiffness is not sensitive to choice of inner ply angle, but choosing an outer ply angle of 30° does result in significant change in torsional stiffness.

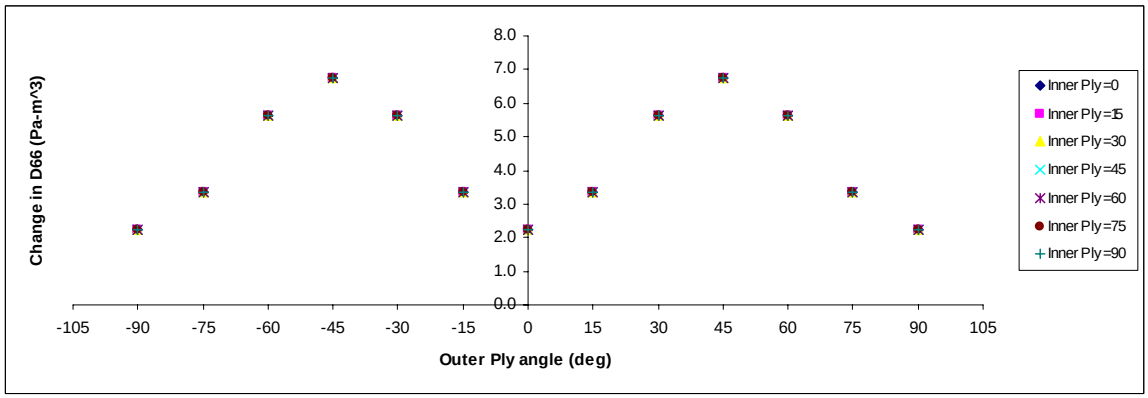

Figure **4-15**: Variation of Change in Torsional Stiffness term in BTM

The terms in the numerator of Equation **4.2** refer to the mean bending and mean torisonal stiffness. It is desired that the value of these terms be high. Figure **4-16** shows the variation in the mean bending stiffness in the coupled and decoupled states for different laminate configurations. The value is symmetric about the x-axis. The sum of the bending stiffness is dependent on the choice of inner ply angle and also on the outer ply angle orientation. It can be seen in Figure **4-16** that choosing an inner ply angle of 30° (yellow dots) produces the third highest value for the sum of bending stiffness. Here the 0° and 15° inner ply angle choice show the highest values of average bending stiffness. But the difference in these values and that obtained using 30° inner ply angle is small. Thus it justifies the BTM's choice of choosing inner plies of 30°. The BTM chooses an outer ply angle of 30°. By observing Figure **4-16**, it can be seen that this choice gives a moderately high value of mean bending stiffness ($D_{11}^{2ply} + D_{11}^{4ply}$).

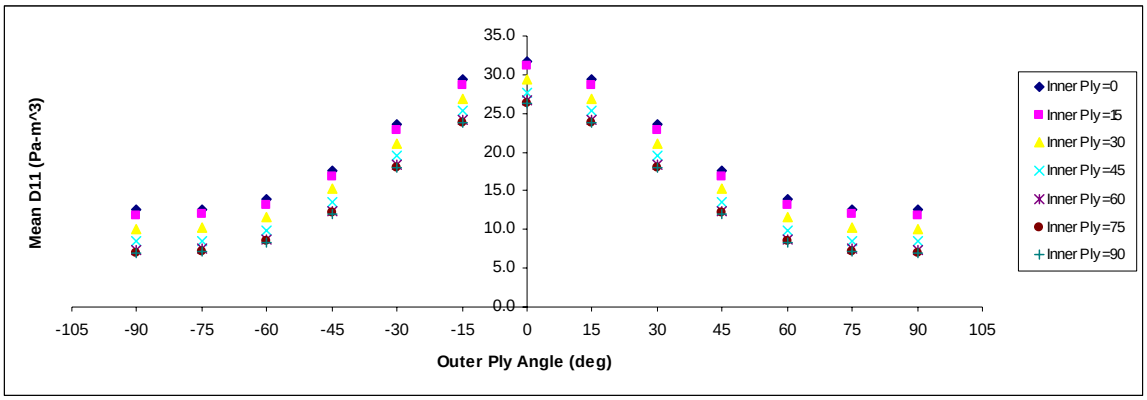

Figure **4-16**: Variation of Mean Bending Stiffness

The mean torsional stiffness in the coupled and decoupled states is plotted in Figure **4-17** for various laminate ply orientations. It can be observed that this term is moderately sensitive to the inner ply angle and relatively more sensitive to the outer ply angle. The value is again symmetric about the y-axis. From Figure **4-17**, choosing an outer ply angle of 30° gives the second highest value for the sum of torsional stiffness. The figure indicates that choosing an inner ply angle of 45° gives a higher value than choosing 30° as the inner ply angle as shown by the BTM. But this difference in value between the inner ply of 45° and 0° is not very significant. Thus it can concluded that the

BTM is not picking the laminate that produces the highest average value of torisonal stiffness but is choosing the second highest value since the difference is small.

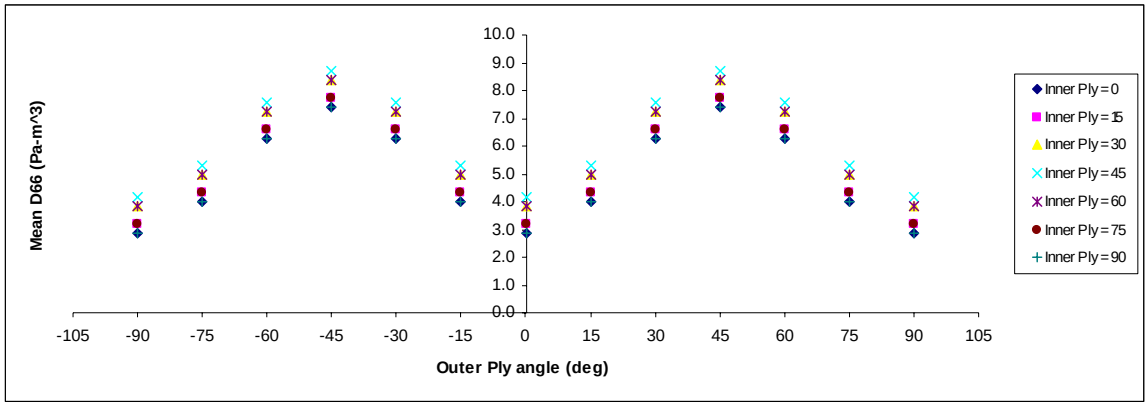

Figure **4-17**: Variation of Mean Torsional Stiffness

Thus the BTM's choice of the **[30/30/30/30]°** laminate is justified since the choice of the outer and inner ply angles correspond to the desired trends in the values of the terms in Equation **4.2**. Overall it is observed that the $(D_{16}^{4ply} - D_{16}^{2ply})$, the $(D_{66}^{4ply} - D_{66}^{2ply})$ and the $(D_{11}^{4ply} - D_{11}^{2ply})$ terms enforce the choice of outer ply angle of 30°, since these terms are independent of inner ply angle orientation. Comparatively the $(D_{11}^{4ply} + D_{11}^{2ply})$ and the $(D_{66}^{4ply} + D_{66}^{2ply})$ terms are more sensitive to inner ply orientation. These terms also drive the BTM to choose the outer ply angle orientation as 30°.

4.2.2 ANSYS Analysis

In order to validate the numerical finite element analysis solution of the extraction of terms in the BTM from the ANSYS solution, the multi-layer beam is first modeled in ANSYS without the inclusion of the polymer layer. Refer to Chapter **3** for details on extraction of BTM terms from ANSYS. Since the Matlab analysis showed that the BTM predicts a maximum value for the **[30/30/30/30]** laminate, the first simulation run in

ANSYS was keeping the inner ply angle as 0° and varying the outer ply angle from -90° to 90°.

In order to extract the parameters required to compute the BTM, two test forces were applied to the beam. First, a bending moment M_{xx} = 1 N-m was applied to the multi-layer beam as shown in Chapter **3**. The tip displacement and bending curvatures were outputted. Second, a torque of M_{xy} = 1 N-m was applied and the tip displacement was outputted. Using these values enabled the calculation of the D_{11}, D_{16}, and D_{66} terms in Equation **4.2**. Note that the ANSYS analysis was first done for inner ply angle of 30˚ and varying outer ply angle thus modeling the ideal 4-ply case.

Thus using the values of D_{11}, D_{16} and D_{66} terms obtained from ANSYS, the BTM was calculated again. The results are shown in Figure **4-18 .** It can be seen that values of the BTM obtained from ANSYS closely match those provided by Matlab for the ideal case, with a 9 % average error. This verifies the validity of the extraction of terms in the ANSYS model as outlined in Chapter **3**.

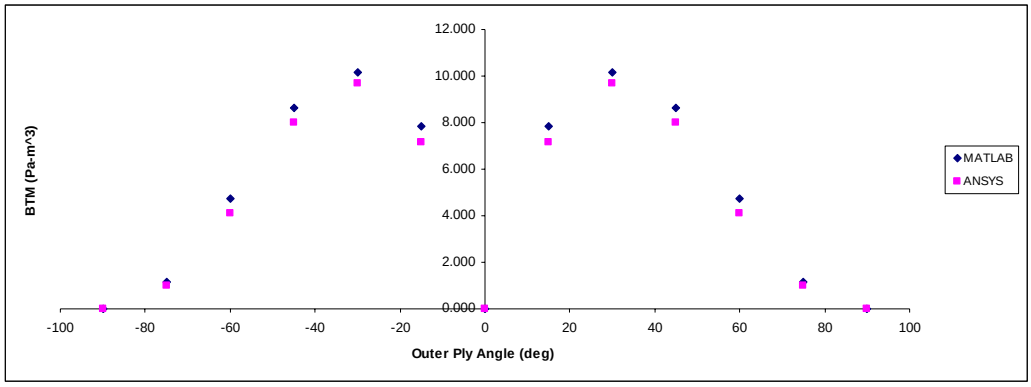

Figure **4-18**: Comparison of Matlab and ANSYS for the [α/30/30/α] laminate

After verifying the accuracy of the terms in the BTM obtained through the ANSYS model, the polymer layers are then introduced in the ANSYS model. To simulate the "glassy" and "rubbery" polymer states respectively, the material properties were assigned to the polymer layer as given in Table **3-2**.

Since the Matlab model indicated the [30/30/30/30] laminate produced the highest value of the BTM, this laminate orientation will be used to model the multi-layered beam

with the polymer layers in ANSYS. The ply thickness is set at 0.5 mm. The presence of the polymer layer thickness affects the results of the analysis. Thus the thickness of the polymer layer was varied as a function of ply thickness till convergence of the BTM solution was obtained. Figure **4-19** shows the BTM with decreasing polymer layer thickness. It can be seen that polymer thickness between 10% to 20% of ply thickness gives a good value of BTM. For thicker polymer layers, coupling between inner and outer plies is not perfect. Thus the thickness of the polymer layer is 0.1 times the ply thickness and is used in the following analysis.

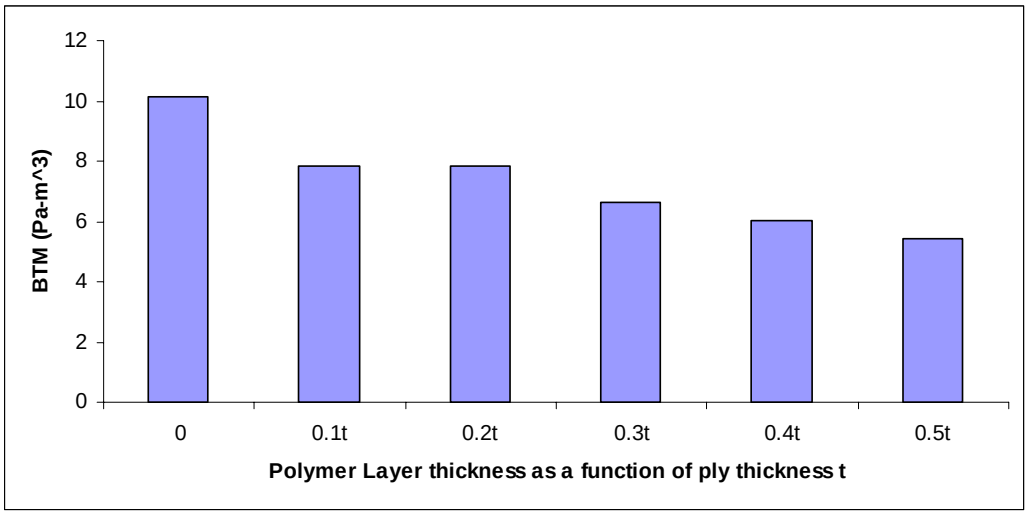

Figure **4-19**: BTM Value as a function of Polymer Thickness for [30/30/30/30] Laminate

In order to adequately depict the shear effects of the polymer layer, the number of solid elements through the polymer layer thickness is increased from one to four elements. As in the ETM case, increasing the number of elements increases computation time but the goal is to obtain a convergent solution or grid independent solution. From this, a convergence study is done which shows the variation of the BTM value with increasing the number of elements through the polymer thickness. Figure **4-20** shows the results of this convergence study. From the figure, again choosing 3 or 4 elements per layer gives a convergent result. In order to reduce computational requirements, 3 elements were used through the polymer layer thickness to model the shear effects of the

polymer layer. Thus 3 elements are used through the thickness of the polymer layer for analysis.

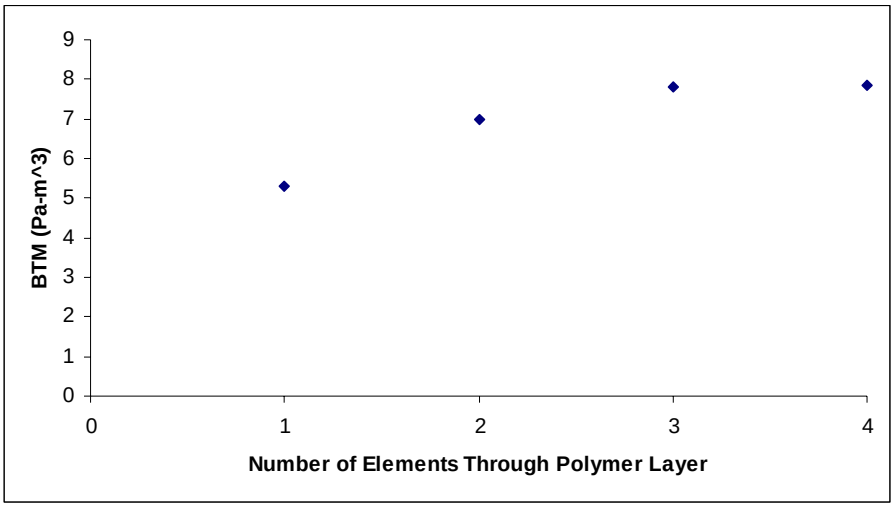

Figure **4-20**: Convergence Study of Varying Number of Elements through Polymer Layer Thickness for the [30/30/30/30] Laminate.

Table **4-2** summarizes the modeling parameters used in the BTM ANSYS model with the polymer layers included. The definition and description of these terms can be found in Chapter **3.3**

Table **4-2**: Summary of BTM ANSYS Modeling Parameters

Parameter	**Value**
Element Type	SOLID 45
Thickness of Polymer Layer	0.05 mm
Mesh Type	Quadrilateral
Mesh Size of Polymer	30 elements along length 30 elements along width 3 elements through thickness
Boundary Conditions	• At x = 0, y , z : u_x, u_y, u_z = 0 (Clamped Boundary Conditions) • At x = 0.254, y , z : F_z (Bending Load)
Outputs	• Displacements: u_x, u_y, u_z

Figure **4-21** shows the comparison of BTM results between Matlab and ANSYS. As discussed in Chapter **3**, in Matlab, a perfect bond assumption is made between the four plies and the Matlab results pertain to a perfectly coupled and decoupled system. In ANSYS the results approach the perfect bond assumption results as can be seen in Figure **4-21**. The blue bar represents the BTM value for the perfectly decoupled case (Matlab Analysis) and the magenta bar represents the BTM value calculated from the ANSYS model. The modulus of the polymer layer was reduced by three orders of magnitude so as to model the 'soft' polymer. The difference in the BTM between ANSYS and Matlab model is due to the effect of the finite thickness and stiffness of the polymer layer modeled in ANSYS. Similar to the ETM case, as expected, the shear effects of the polymer layer tend to decouple the system, but due to the polymer's finite thickness and stiffness, the inner two plies are never completely decoupled from the outer two plies.

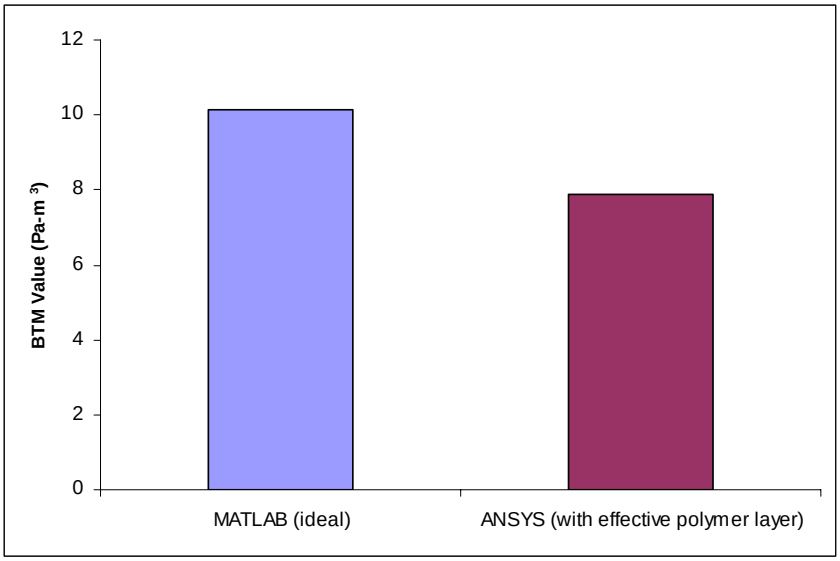

Figure **4-21**: Comparison of BTM between Matlab and ANYS model with polymer layers for the [30/30/30/30] laminate

The ETM is highly dependent on the coupling parameter terms. Similarly the BTM too is highly dependent on the coupling parameters such as D_{16}. As the polymer

went through its glass transition and the beam outer layers were decoupled. The laminate is chosen as **[-30/30/30/-30]** for the purpose of illustration. It still will have the highest BTM value because the BTM is symmetric about the y-axis as described earlier and the outer ply angles both can be -30° or +30 °. The lay-up is still symmetric so as to exhibit bending-twist coupling.

Hence Figure **4-22** shows the comparison in the coupling parameter D_{16} between the glassy and rubbery polymer states respectively. The blue bars represent the ideal Matlab state. An interesting observation here is that the D_{16} term changes sign when the polymer layer transitions from glassy to rubbery state. This indicates that the tip twist in the multi-layered beam changes direction when the polymer is in the low shear modulus rubbery state. Thus in the coupled state the tip twist is dominated by the outer plies, but in the decoupled state, the opposite sign inner plies dominate the tip twist behavior and thus change in sign of tip twist is obtained.

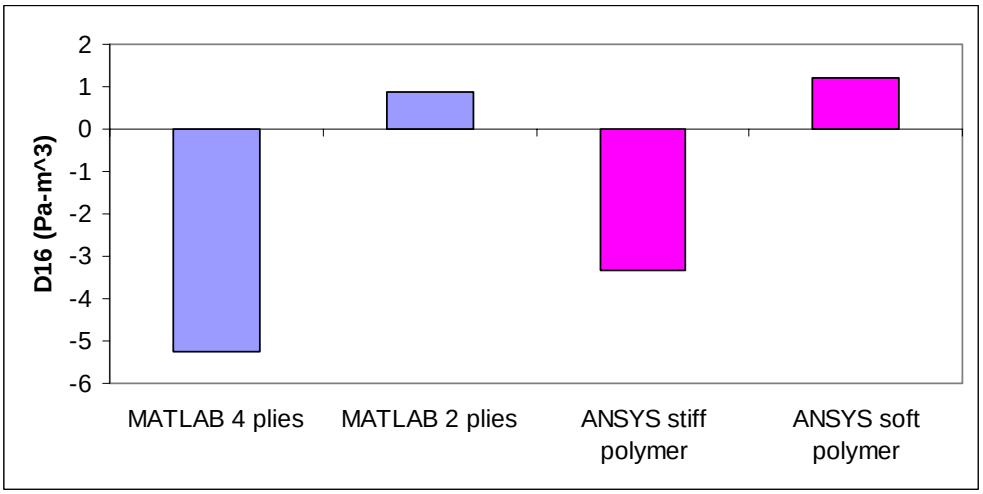

Figure **4-22**: Comparison of ANSYS and Matlab D_{16} results for [-30/30/30/-30] laminate

The pink bars represent the ANSYS model calculation of D_{16}. In the 4-ply case, the value of the coupling parameter is high when the polymer layer is stiff. But when the polymer layer is in the 'soft' state, since the inner plies are not completely decoupled

from the outer plies, the influence of the outer plies affects the coupling parameter in the soft polymer state. This is evident from Figure **4-22**. When the polymer is soft, the coupling term in the last pink bar does not change as that predicted by Matlab (2^{nd} blue bar). This indicates that the presence of the finite thickness polymer layer affects the couplings of the system.

Chapter 5

CONCLUSIONS

This chapter presents and discusses the conclusions then are drawn from the basis of the study presented so far. Firstly, conclusions regarding the development and feasibility of the Extension-Twist and Bending Twist Metrics are presented. Secondly, conclusions are drawn from the modeling approach used in this study. The effects of the finite stiffness and thickness of the polymer layer are discussed as well. This is followed by some recommendations for future work in this study and also recommendations on possible experimental solutions.

5.1 Metrics

The overall objective of this study was to explore the feasibility of composites in controllable structures using the thermal softening properties of polymers. This objective was met through identification, analysis and development of metrics. Since elastic tailoring of composite structures, namely the effects associated with extension-twist coupling and bending-twist coupling is a topic of great interest, it was apparent that these metrics developed needed to encapsulate the coupling characteristics.

In the case of extension-twist coupling, this was accomplished by involving the change in the coupling stiffness parameter B_{16} in the metric. Thus the difference in coupling between the 4 ply coupled state and the 2 ply decoupled state was observed. The Extension-Twist Metric (ETM) also needed to define a laminate that had large change in couplings but at the same time ensuring that the extensional and torsional stiffness of the multi-layered beam were not adversely affected due to the decoupling of the inner plies from the outer plies. Thus the ETM was defined such that the difference in the extensional stiffness terms between the coupled and decoupled states was a minimum. Similarly the difference in torsional stiffness was also minimized. In addition the sum of

the extensional stiffness in the coupled and decoupled states was maximized. So was the sum of the torsional stiffness.

Thus the ETM was successful in quantifying the couplings of the beam as well as relating it to the extensional and torsional stiffness of the structure. Through a detailed laminate analysis, the ETM predicted that choosing a lay-up of [-45/0/0/45]° laminate would exhibit the greatest change in coupling between the coupled and decoupled states but at the same time also ensure the structural integrity of the beam. This laminate produced the highest numerical value for the ETM. Further analysis in each term of the ETM supported the ETM's choice for the [-45/0/045] ° laminate.

To quantify the effects of bending-twist coupling, another metric was developed. This metric is referred to as Bending-Twist Metric (BTM). In this metric, the goal was to maximize the change in the coupling term D_{16} between the 4-ply coupled and the 2-ply decoupled states. The BTM was defined having a large change in bending twist coupling but a low change in bending and torsional stiffness. This is to ensure that the fundamental stiffness' i.e. bending and torsional stiffness were not adversely affected due to the decoupling of the inner plies from the outer plies. Thus the BTM defined the change in couplings to be maximized and simultaneously minimizing the change in bending and tosrional stiffness. In order to ensure that the average stiffness of the structure was not drastically changed, the sum of the bending stiffness in the coupled and decoupled states was also included in the BTM. This sum was to be maximized. Similarly the sum of the torsional stiffness in the coupled and decoupled states was also maximized.

The BTM was successful in quantifying the couplings associated with the multi-layered beam as well as ensuring structural integrity. Through a detailed laminate analysis, the BTM predicted that the choice of a [30/30/30/30]° laminate would exhibit the greatest change in coupling between the coupled and decoupled states but also at the same time ensure that the change in bending and torsional stiffness respectively were minimized. This laminate produced the highest value of the ETM. Further analysis of each term in the BTM indicated that the metric was indeed attempting to pick the lay-up that had high change in coupling but low changes in bending and torsional stiffness respectively.

Both the ETM and BTM equations were successful in designing a multi-layer composite beam that was able to exhibit elastic couplings without adversely altering the fundamental extensional, bending and torsional stiffness of the structure.

5.2 Modeling

One of the objectives of this research was to perform studies of various laminate stacking sequences to obtain the maximum values for the ETM and BTM respectively. A model was developed in Matlab to perform these laminate studies by varying the outer and inner ply angle orientations. In order to identify the theoretical extremes of the system, namely perfectly coupled and perfectly decoupled, the Matlab model assumed that the multi-layered beam was effectively a 2 ply system in the decoupled state. CLPT was used to model the layers in Matlab.

Through the Matlab model, the A, B and D stiffness matrices were obtained for the perfectly coupled 4-ply system and then for the perfectly decoupled 2-ply system. From these matrices, the appropriate terms were extracted and used in the calculation of the ETM and the BTM. Thus the ETM and BTM values calculated from the Matlab model are the theoretical maximum values that could be obtained if the polymer was infinitesimally thin.

A finite element model was developed in ANSYS software to include the polymer layer and its shear kinematics which cannot be captured by the CLPT Matlab model. Solid elements were used to model the composite layers and the polymer layer. The clamped boundary conditions were modeled on the left end of the beam and the applied loads (axial, bending and torsion) were applied to the right end. The ANSYS model was able to output the displacements in all directions as well as the strains. From these outputs, tip twists and bending curvatures could be calculated. Through analysis, these values were used to compute the terms of the ETM and the BTM.

Studies indicated that the value of the ETM and the BTM approach the ideal when the polymer thickness is modeled as one-tenth of the composite ply thickness. Also, through convergence tests, it was determined that having 3 solid elements though the thickness of each layer lead to convergence in the ETM and BTM value. The model utilized a quadrilateral mesh element shape with 30 elements along the length and width of the multi-layered beam.

In order to confirm the accuracy of the ANSYS model in outputting the stiffness terms, an analysis was run using a perfectly decoupled and coupled 2-ply and 4-ply system model respectively (no polymer layer modeled). The ETM and BTM were calculated from the finite element model at these theoretical extremes. The ETM value obtained by Matlab agreed with that obtained by this finite element model with an error of about 4%. This error is attributed to the shear being modeled in the ANSYS model. The BTM value agreed with an error of about 9%. Again this can be attributed to the shear being modeled by the solid elements.

The value of the ETM obtained by the finite element model approached the value obtained by the perfect bond assumption model in Matlab. This shows that the polymer layer's presence is a limiting factor in completely decoupling the system. However, it is the change in shear modulus of the polymer layer with temperature that indeed enables the decoupling of the inner plies from the outer plies. The fact that the ETM value generated by the finite element model approaches the Matlab model value is an indication that the change by 3 orders of magnitude of the polymer modulus is providing a change in coupling to the system. Due to the polymer's finite thickness and stiffness, the inner plies are never completely decoupled from the outer plies. In the BTM case, the value also approached that obtained by the Matlab model. Again this indicates that the polymer layer, through variation in its shear modulus is able to decouple the system. This also concludes that the effect of change in bending-twist coupling is captured by the finite element model in the presence of the polymer layer. Also as in the case of the ETM, the BTM value generated by the finite element model will always be lower than the perfect bond Matlab model since the finite thickness and stiffness of the polymer do not allow for the inner plies to be completely decoupled from the outer plies.

Overall, it is important to conclude that these metrics have enabled the design of a composite laminate structure whose stiffness and couplings can be controlled by the use of a compliant polymer layer. The variation in shear modulus of the polymer acts as a decoupling medium which in turn acts a variable stiffness controlling material. Thus the highly desired aero-elastic effects of composite materials can be in a variable stiffness structure and the metrics ensure that the structure does not lose its fundamental stiffness and continues to act as a useful load bearing structure.

5.3 Recommendations for Future Work

Through the completion of this research, much insight was gained from the development of metrics, detailed laminate analysis and modeling of the multi-layer composite beam. Employing this insight, recommendations are provided for future work in this area or reacted areas of research. These recommendations also include experimental analysis that wasn't conducted here.

1. In order to demonstrate the decoupling mechanism of the polymer layer, the composite plies and the polymer need to be fabricated separately. In order to fabricate angled plies using graphite/epoxy, it is easier to adopt fabrication methods using prepregs. Heating pads to heat the polymer need to be able to provide temperatures ranging from room temperature to more than 350° F since most commercially available polymers do not change their modulus by 3 orders of magnitude when heated between room temperature and the 300° F range. The best alternative would be to fabricate the polymer in a facility. High temperature adhesive glue would be required to bond the polymer layers to the composite plies.
2. In order to demonstrate the change in coupling by polymer stiffness variation, sensitive tensile and loading machines should be used. Since tip twists and displacements obtained are usually very small in magnitude, highly sensitive devices such as optical sensors, LVDTs or strain gages

should be used and can be placed at the tips of the free end of the beam. Failure analysis will precede the experimental data acquisition in order to ensure the laminate does not fail during testing.

3. Identify applications of the current study in aerospace systems where changes in couplings would be beneficial.
4. Quantify the energy requirements to realize change in couplings in multi-layered beams.
5. Explore non-thermal methods to reduce the shear modulus of the polymer interface layer (example: using a light activated shape memory polymer) instead of heating of a regular polymer though glass transition.

Bibliography

1. Onoda J., Endo T., Tamaoki H. and Watanabe N., "Vibration suppression by variable-stiffness members", *AIAA J. 29*, 977-83, 1991.

2. Yong C., Zimcik D. G., Wickramasinghe V. K. and Nitzsche F., "Development of the smart spring for active vibration control of helicopter blades", *Journal of Intelligent Material Systems and Structures*, Vol. 15, 37-47, 2004.

3. Gandhi, F., Anusonti-Inthra, P., "Adaptive control of semi-active variable stiffness devices for narrow band disturbance rejection", *Journal of Intelligent Material Systems and Structures*, Vol. 14, 191-201, 2003.

4. Davis C. L., Lesieutre G.A., "An actively tuned solid state vibration absorber using capacitive shunting of piezoelectric stiffness", *Journal of Sound and Vibration*, Vol. 232, 601-6127, 2000.

5. Clark, W.W., "Vibration control with state switching piezoelectric materials", *Journal of Intelligent Material Systems and Structures*, Vol. 11, 263-271, 2000.

6. Corr, L. R., and Clark, W.W., "Comparison of low frequency piezoelectric switching shunt techniques for structural damping", *Journal of Smart Materials and Structures*, Vol. 11, 370-376, 2002.

7. Otsuka K., Wayman C. M., "Shape Memory Materials", 1st Edition, *Cambridge University Press*, pp 203-219, 1998.

8. Hodgson D. E., "Using Shape Memory Alloys", Sunnyvale, CA: Shape Memory Applications.

9. Wei Z. G., Sandstrom R., Miyazaki S., "Review: Shape memory materials and hybrid composites for smart systems", *Journal of Material Sciences*, Vol. 33, 3743-3762, 1998.

10. Lendlein A., Kelch S., "Shape memory polymers", *Agnew. Chem. Int. Edn* , Vol. 41, 2034-2057, 2002.

11. Atli, B., Gandhi, F., and Karst, G., "Thermomechanical Characterization of Shape Memory Polymers", *Proceedings of the SPIE*, Vol. 6524, 2007.

12. Perkins D. A., Reed J. L. Jr, Havens E., "Adaptive wing structures", Smart Structures and Materials, Industrial and Commercial Applications of Smart Structures Technologies; *Proc. SPIE* Vol. 5388, 225-233, 2004.

13. Reed J. L. Jr, Hemmelgarn C. D., Pelley B. M., Havens E., "Adaptive wing structures", Smart Structures and Materials, Industrial and Commercial Applications of Smart Structures Technologies; *Proc. SPIE* Vol. 5762 132-142, 2005.

14. Gandhi, F., Kang, Sang-Guk, "Beams with controllable flexural stiffness", *Proceedings of the SPIE*, Vol. 6525, 2007.

15. Gandhi F., Kang S., "Beams with controllable flexural stiffness", *Journal of Smart Materials and Structure*s, Vol. 16, 1179-1184, 2007.

16. Hong C. H., Chopra I., "Aeroelastic stability of a composite rotor blade", *Journal of The American Helicopter Society*, Vol. 30, N0. 2, pp 57-67, 1985.

17. Panda B., Chopra I., "Dynamics of composite rotor blades in forward flight", *Vertica*, Vol. 11, 187-209, 1987.

18. Kosmatka J. B., "Extension-bend-twist coupling behavior of nonhomogenous anisotropic beams with initial twist", *Proceedings of the 32nd Structures, Structural Dynamics and Materials Conference*, Baltimore, MD, 1037-1049, 1991.

19. Kosmatka J. B., Lake R. C., "Extension-twist behavior of initially twisted composite spars for tilt-rotor applications", *Proceedings of the 37th Structures, Structural Dynamics and Materials Conference*, Salt Lake City, Utah, Vol. 4, 2175-2184, 1996.

20. Nampy S.N., Smith, E., "Extension twist coupled tilt rotor blades using flexible matrix composites", *46th AIAA/AHS/ASME/ASCE/ASC Structures, Structural Dynamics and Materials Conference*, Vol. 2152, 2005.

21. Kosmatka John B., Nixon M. W., Piatak David J., "Stiffness characteristics of rotor blades with composite couplings", NASA technical paper 3641, ARL technical report 1279, 1997.

22. Narayanan Nampy S., "Structural Behavior and Design of Flexible Matrix Composite Box Beams with Extension-twist Coupling". M.S. Thesis, Pennsylvania State Univ., University Park, PA, 2005.

23. Lake R.C., Nixon M.W., Wilbur J.D., Singleton., Mirick P.H., "A demonstration of passive blade twist control using extension-twist couplings", *Proceedings of the 33rd Structures, Structural Dynamics and Materials Conference*, Dallas, TX, 1992.

24. Nixon M. W., "Analytical and Experimental Investigations of Extension-Twist coupled Structures", M.S. Thesis, George Washington University, Hampton, VA, 1989.

25. Chandra R., Chopra I., "Experimental and Theoretical Analysis of Composite I-beams with Elastic Couplings", *Proceedings of the 32nd AIAA Structures, Structural Dynamics and Materials Conference*, Baltimore, MD, 1050-1067, 1991.

26. Khan A. M., Adams D. O., Dayal V., Vogel J. M., "Effect of bending-twist coupling on composite propeller blade performance", *Mechanics of Composite Materials and Structures*, Vol. 7, No. 4, 383-401, 2000.

27. Nixon M. W., "Extension-Twist Coupling of Composite Circular Tubes with Application to Tiltrotor Blade Design", *Proceedings of the 28th AIAA Structures, Structural Dynamics and Materials Conference*, AIAA paper No. 87-0772, Monterey, CA, 295-303, 1987.

28. Ozbay S., "Extension-Twist Coupling Optimization in Composite Rotor Blades", Diss., Georgia Institute of Technology, GA, 2005.

29. Reddy, J.N., "Mechanics of laminated composite plates and shells: theory and analysis", 2nd edition, Boca Raton: CRC press, 2004.

30. Juska T., "Fabrication Methods." Penn State University. Composites Process. University Park, PA, 15 Mar. 2007.

31. "ANSYS Solid 191 Element Description", ANSYS Inc, 2008.

Appendix A

Stiffness Matrices from Classical Laminated Plate Theory

A.1 Definition of Terms

E_1	= Young's Modulus along longitudinal fiber direction
E_2	= Young's Modulus in the transverse direction
G_{12}	= Shear Modulus
ν_{12}	= Poisson's Ratio
θ	= Fiber orientation with respect to the laminate axis
$\sigma_{xx}, \sigma_{yy}, \sigma_{xy}$	= Tensile stress, transverse stress, in-plane shear stress
$\varepsilon_{xx}, \varepsilon_{yy}, \varepsilon_{xy}$	= Tensile strain, transverse strain, in-plane shear strain
ε^0	= Strain at the mid-point of laminate
$\kappa_{xx}, \kappa_{yy}, \kappa_{xy}$	= Bending, transverse and twist curvature
z	= Axis along the laminate thickness
t	= Thickness of laminate
U	= Strain energy
A_{11}	= Extensional Stiffness
B_{16}	= Extension-Twist Coupling Stiffness
D_{11}	= Bending Stiffness
D_{66}	= Torsional Stiffness

A.2 Stiffness Coefficients

As shown in Figure **A-1,** fibers in a laminated composite plate can be oriented along a particular direction with respect to the laminate axes (x, y). The (1-2) directions are perpendicular to the fiber and they are defined as the principal axes of the orthotropic ply. In an orthotropic material, the properties, especially the Young's modulus along fiber is much greater than along the matrix direction. Here there are four independent constants namely E_1, E_2, ν, and G_{12}.

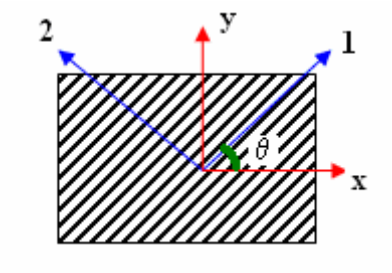

Figure **A-1**: Ply axis and Laminate Axis

In plate theory, stresses and strains and thus stress-strain relationships in ply axis can be transformed to the laminate axis by using a transformation matrix. Thus the stress-strain relation in the laminate axis can be written as:

$$\begin{Bmatrix} \sigma_{xx} \\ \sigma_{yy} \\ \sigma_{xy} \end{Bmatrix} = \begin{bmatrix} \overline{Q}_{11} & \overline{Q}_{12} & \overline{Q}_{16} \\ \overline{Q}_{12} & \overline{Q}_{22} & \overline{Q}_{26} \\ \overline{Q}_{16} & \overline{Q}_{26} & \overline{Q}_{66} \end{bmatrix} \begin{Bmatrix} \varepsilon_{xx} \\ \varepsilon_{yy} \\ \varepsilon_{xy} \end{Bmatrix}$$

where

$$\overline{Q}_{11} = Q_{11}\cos^4\theta + Q_{22}\sin^4\theta + 2(Q_{12} + 2Q_{66})\sin^2\theta\cos^2\theta$$
$$\overline{Q}_{22} = Q_{11}\sin^4\theta + Q_{22}\cos^4\theta + 2(Q_{12} + 2Q_{66})\sin^2\theta\cos^2\theta$$
$$\overline{Q}_{12} = (Q_{11} + Q_{22} - 4Q_{66})\sin^2\theta\cos^2\theta + Q_{12}(\sin^4\theta + \cos^4\theta)$$
$$\overline{Q}_{66} = (Q_{11} + Q_{22} - 2Q_{12} - 2Q_{66})\sin^2\theta\cos^2\theta + Q_{66}(\sin^4\theta + \cos^4\theta)$$
$$\overline{Q}_{16} = (Q_{11} - Q_{12} - 2Q_{66})\sin\theta\cos^3\theta - (Q_{22} - Q_{12} - 2Q_{66})\sin^3\theta\cos\theta$$
$$\overline{Q}_{26} = (Q_{11} - Q_{12} - 2Q_{66})\sin^3\theta\cos\theta - (Q_{22} - Q_{12} - 2Q_{66})\sin\theta\cos^3\theta$$

where Q terms are the material stiffness matrix terms

$$Q_{11} = \frac{E_1}{1-\nu_{12}\nu_{21}}\ ,\ Q_{22} = \frac{E_2}{1-\nu_{12}\nu_{21}},\ Q_{66} = G_{12},\quad Q_{12} = \frac{\nu_{12}E_2}{1-\nu_{12}\nu_{21}} = \frac{\nu_{21}E_1}{1-\nu_{12}\nu_{21}}$$

Thus the stresses and strains in the laminate axes are given as:

$$\begin{Bmatrix}\sigma_{xx}\\ \sigma_{yy}\\ \sigma_{xy}\end{Bmatrix} = \overline{Q}\begin{Bmatrix}\varepsilon_{xx}\\ \varepsilon_{yy}\\ \varepsilon_{xy}\end{Bmatrix}$$

Strains in the laminate axis can be written as a function of mid-plane strains and curvatures as follows.

$$\begin{Bmatrix}\varepsilon_{xx}\\ \varepsilon_{yy}\\ \varepsilon_{xy}\end{Bmatrix} = \begin{Bmatrix}\varepsilon^0{}_{xx}\\ \varepsilon^0{}_{yy}\\ \varepsilon^0{}_{xy}\end{Bmatrix} + z\begin{Bmatrix}\kappa_{xx}\\ \kappa_{yy}\\ \kappa_{xy}\end{Bmatrix}$$

Strain Energy is expressed as:

$$U = \frac{1}{2}\int_{Volume} \begin{bmatrix} \varepsilon_{xx} & \varepsilon_{yy} & \varepsilon_{xy} \end{bmatrix} \begin{Bmatrix} \sigma_{xx} \\ \sigma_{yy} \\ \sigma_{xy} \end{Bmatrix} dV$$

$$In\,the\,ply\,axes\,system\,(\tilde{x},\tilde{y})$$

$$U = \frac{1}{2}\int_{Volume} \begin{bmatrix} \tilde{\varepsilon}_0^T & \tilde{\kappa}^T \end{bmatrix} \begin{bmatrix} \tilde{\bar{Q}} & z\tilde{\bar{Q}} \\ z\tilde{\bar{Q}} & z^2\tilde{\bar{Q}} \end{bmatrix} \begin{Bmatrix} \tilde{\varepsilon}_0 \\ \tilde{\kappa} \end{Bmatrix} dzdA$$

Integrate though the thickness (z direction)

$$\int_{-t/2}^{t/2} \tilde{\bar{Q}}\,dz = \tilde{A}$$

$$\int_{-t/2}^{t/2} z^2\tilde{\bar{Q}}\,dz = \tilde{D}$$

$$\int_{-t/2}^{t/2} z\tilde{\bar{Q}}\,dz = \tilde{B}$$

Thus

$$U = \frac{1}{2}\iint_{Area} \begin{bmatrix} \tilde{\varepsilon}_0^T & \tilde{\kappa}^T \end{bmatrix} \begin{bmatrix} \tilde{A} & \tilde{B} \\ \tilde{B} & \tilde{D} \end{bmatrix} \begin{Bmatrix} \tilde{\varepsilon}_0 \\ \tilde{\kappa} \end{Bmatrix}$$

The A, D and B matrices are the Extensional in-plane stiffness, Bending stiffness and Extension/Bending Coupling stiffness respectively. For a laminated composite $\bar{Q}$ can differ from ply to ply. Defining the Force and Moment Resultants as:

N_x = Resultant Force in the x-direction (per unit length in the y-direction)

N_y = Resultant Force in the y-direction (per unit length in the x-direction)\

N_{xy} = Shear Force

M_x = Resultant moment about the y-axis (per unit length in y-direction)

M_y = Resultant moment about the x-axis (per unit length in x-direction)

M_{xy} = Twisting Moment

The Force Resultants can be written in the form of the *A* and *B* matrices as follows:

$$\begin{Bmatrix} N_x \\ N_y \\ N_{xy} \end{Bmatrix} = [A] \begin{Bmatrix} \varepsilon^0{}_{xx} \\ \varepsilon^0{}_{yy} \\ \varepsilon^0{}_{xy} \end{Bmatrix} + [B] \begin{Bmatrix} \kappa_{xx} \\ \kappa_{yy} \\ \kappa_{xy} \end{Bmatrix}$$

Similarly, the Moment Resultants can be expressed in terms of the *B* and *D* matrices as shown below:

$$\begin{Bmatrix} M_x \\ M_y \\ M_{xy} \end{Bmatrix} = [B] \begin{Bmatrix} \varepsilon^0{}_{xx} \\ \varepsilon^0{}_{yy} \\ \varepsilon^0{}_{xy} \end{Bmatrix} + [D] \begin{Bmatrix} \kappa_{xx} \\ \kappa_{yy} \\ \kappa_{xy} \end{Bmatrix}$$

Combining the Force and Moment Resultants gives:

$$\begin{Bmatrix} N_x \\ N_y \\ N_{xy} \\ M_x \\ M_y \\ M_{xy} \end{Bmatrix} = \begin{bmatrix} A_{11} & A_{12} & A_{16} & B_{11} & B_{12} & B_{16} \\ A_{12} & A_{22} & A_{26} & B_{12} & B_{22} & B_{26} \\ A_{16} & A_{26} & A_{66} & B_{16} & B_{26} & B_{66} \\ B_{11} & B_{12} & B_{16} & D_{11} & D_{12} & D_{16} \\ B_{12} & B_{22} & B_{26} & D_{21} & D_{22} & D_{26} \\ B_{16} & B_{26} & B_{66} & D_{16} & D_{26} & D_{66} \end{bmatrix} \begin{Bmatrix} \varepsilon^0_{xx} \\ \varepsilon^0_{yy} \\ \varepsilon^0_{xy} \\ \kappa_{xx} \\ \kappa_{yy} \\ \kappa_{xy} \end{Bmatrix}$$

$$\Rightarrow \begin{Bmatrix} \widetilde{N} \\ \widetilde{M} \end{Bmatrix} = \begin{bmatrix} \widetilde{A} & \widetilde{B} \\ \widetilde{B} & \widetilde{D} \end{bmatrix} \begin{Bmatrix} \widetilde{\varepsilon}^0 \\ \widetilde{\kappa} \end{Bmatrix}$$

Appendix B

MATLAB Laminate Analysis Computer Program

```
%*************************************************************************
%CLPT Laminate Ply Analysis Extraction of A,B,D Stiffness Matrices
        %Author: Alvord Marques
%Last Modified: 07/01/2008
%*************************************************************************
clear all
format short g

%Define Ply angle orientation and layup
teta1=   -45*pi/180;
teta2=  30*pi/180;
teta3=  -30*pi/180;
teta4=  -45*pi/180;

%Define Material Properties
E11=138e9;
E22=8.96e9;
G12=7.89e9;
mu12=0.32;
mu21=(E22/E11)*mu12;

%Define beam Dimensions
th= 0.5e-3; % thickness
L=0.254;
b=5.08e-2;

%Calculate Stiffnes Coefficients
dela= 1-mu12*mu21;

Q=[ E11/dela mu12*E22/dela 0; mu12*E22/dela E22/dela 0; 0 0 G12];

Q11=Q(1,1);
```

```
Q12=Q(1,2);
Q22=Q(2,2);
Q66=Q(3,3);

% To get the elements of the Q11-bar matrix
Q11_teta1= Q11*cos(teta1)^4 + (2*(Q12+2*Q66)*sin(teta1)^2)*cos(teta1)^2     + Q22*sin(teta1)^4;

Q11_teta2= Q11*cos(teta2)^4 + (2*(Q12+2*Q66)*sin(teta2)^2)*cos(teta2)^2 + Q22*sin(teta2)^4;
Q11_teta3= Q11*cos(teta3)^4 + (2*(Q12+ 2*Q66)*sin(teta3)^2)*cos(teta3)^2 + Q22*sin(teta3)^4;
Q11_teta4= Q11*cos(teta4)^4 + (2*(Q12 +   2*Q66)*sin(teta4)^2)*cos(teta4)^2 + Q22*sin(teta4)^4;

%To get the elements of the Q12-bar matrix
Q12_teta1= (Q11 + Q22 - 4*Q66)*sin(teta1)^2*(cos(teta1)^2)+ Q12*(sin(teta1)^4 + cos(teta1)^4);
Q12_teta2= (Q11 + Q22 - 4*Q66)*sin(teta2)^2*(cos(teta2)^2)+ Q12*(sin(teta2)^4 + cos(teta2)^4);
Q12_teta3= (Q11 + Q22 - 4*Q66)*sin(teta3)^2*(cos(teta3)^2)+ Q12*(sin(teta3)^4 + cos(teta3)^4);
Q12_teta4= (Q11 + Q22 - 4*Q66)*sin(teta4)^2*(cos(teta4)^2)+ Q12*(sin(teta4)^4 + cos(teta4)^4);


%To get the elemnents of the Q22-bar Matrix
Q22_teta1= Q11*sin(teta1)^4 + 2*(Q12 + 2*Q66)*sin(teta1)^4*(cos(teta1)^4) + Q22*cos(teta1)^4;
Q22_teta2= Q11*sin(teta2)^4 + 2*(Q12 + 2*Q66)*sin(teta2)^4*(cos(teta2)^4) + Q22*cos(teta2)^4;
Q22_teta3= Q11*sin(teta3)^4 + 2*(Q12 + 2*Q66)*sin(teta3)^4*(cos(teta3)^4) + Q22*cos(teta3)^4;
Q22_teta4= Q11*sin(teta4)^4 + 2*(Q12 + 2*Q66)*sin(teta4)^4*(cos(teta4)^4) + Q22*cos(teta4)^4;


%To get the elements of Q16-bar matrix
Q16_teta1= (Q11-Q12-2*Q66)*sin(teta1)*cos(teta1)^3 + (Q12 - Q22 + 2*Q66)*sin(teta1)^3*(cos(teta1));
Q16_teta2= (Q11-Q12-2*Q66)*sin(teta2)*cos(teta2)^3 + (Q12 - Q22 + 2*Q66)*sin(teta2)^3*(cos(teta2));
Q16_teta3= (Q11-Q12-2*Q66)*sin(teta3)*cos(teta3)^3 + (Q12 - Q22 + 2*Q66)*sin(teta3)^3*(cos(teta3));
Q16_teta4= (Q11-Q12-2*Q66)*sin(teta4)*cos(teta4)^3 + (Q12 - Q22 + 2*Q66)*sin(teta4)^3*(cos(teta4));

%To get elements of Q26-bar matrix
Q26_teta1= (Q11-Q12-2*Q66)*sin(teta1)^3*cos(teta1) + (Q12 - Q22 + 2*Q66)*sin(teta1)*(cos(teta1)^3);
Q26_teta2= (Q11-Q12-2*Q66)*sin(teta2)^3*cos(teta2) + (Q12 - Q22 + 2*Q66)*sin(teta2)*(cos(teta2)^3);
Q26_teta3= (Q11-Q12-2*Q66)*sin(teta3)^3*cos(teta3) + (Q12 - Q22 + 2*Q66)*sin(teta3)*(cos(teta3)^3);
Q26_teta4= (Q11-Q12-2*Q66)*sin(teta4)^3*cos(teta4) + (Q12 - Q22 + 2*Q66)*sin(teta4)*(cos(teta4)^3);
```

```
%To get the elements of the Q66-bar matrix
Q66_teta1= (Q11+Q22-2*Q12 - 2*Q66)*sin(teta1)^2*cos(teta1)^2 + Q66*(sin(teta1)^4 + cos(teta1)^4);
Q66_teta2= (Q11+Q22-2*Q12 - 2*Q66)*sin(teta2)^2*cos(teta2)^2 + Q66*(sin(teta2)^4 + cos(teta2)^4);
Q66_teta3= (Q11+Q22-2*Q12 - 2*Q66)*sin(teta3)^2*cos(teta3)^2 + Q66*(sin(teta3)^4 + cos(teta3)^4);
Q66_teta4= (Q11+Q22-2*Q12 - 2*Q66)*sin(teta4)^2*cos(teta4)^2 + Q66*(sin(teta4)^4 + cos(teta4)^4);

%Writing in Matrix form as a row matrix
Q11_bar= [ Q11_teta1 Q11_teta2 Q11_teta3 Q11_teta4];
Q12_bar= [ Q12_teta1 Q12_teta2 Q12_teta3 Q12_teta4];
Q22_bar= [ Q22_teta1 Q22_teta2 Q22_teta3 Q22_teta4];
Q16_bar= [ Q16_teta1 Q16_teta2 Q16_teta3 Q16_teta4];
Q26_bar= [ Q26_teta1 Q26_teta2 Q26_teta3 Q26_teta4];
Q66_bar= [ Q66_teta1 Q66_teta2 Q66_teta3 Q66_teta4];

% AMatrix
A11=th*(Q11_teta1 + Q11_teta2 + Q11_teta3 + Q11_teta4 );
A12=th*( Q12_teta1+ Q12_teta2+ Q12_teta3 +Q12_teta4);
A22=th*(Q22_teta1 +Q22_teta2+ Q22_teta3 +Q22_teta4);
A16=th*(Q16_teta1 +Q16_teta2 +Q16_teta3+ Q16_teta4);
A26=th*(Q26_teta1 +Q26_teta2 +Q26_teta3 +Q26_teta4);
A66=th*(Q66_teta1 +Q66_teta2 +Q66_teta3 +Q66_teta4);

A=[A11 A12 A16; A12 A22 A26; A16 A26 A66]

% B matrix
%Defining zkbar
zkbar1=1.5*th;
zkbar2=0.5*th;
zkbar3=0.5*th;
zkbar4=1.5*th;

B11= Q11_teta1*th*zkbar1+Q11_teta2*th*zkbar2-Q11_teta3*th*zkbar3 - Q11_teta4*th*zkbar4;
B12= Q12_teta1*th*zkbar1+Q12_teta2*th*zkbar2-Q12_teta3*th*zkbar3 - Q12_teta4*th*zkbar4;
B16= Q16_teta1*th*zkbar1+Q16_teta2*th*zkbar2-Q16_teta3*th*zkbar3 - Q16_teta4*th*zkbar4;
B22= Q22_teta1*th*zkbar1+Q22_teta2*th*zkbar2-Q22_teta3*th*zkbar3 - Q22_teta4*th*zkbar4;
B26= Q26_teta1*th*zkbar1+Q26_teta2*th*zkbar2-Q26_teta3*th*zkbar3 - Q26_teta4*th*zkbar4;
B66= Q66_teta1*th*zkbar1+Q66_teta2*th*zkbar2-Q66_teta3*th*zkbar3 - Q66_teta4*th*zkbar4;
```

```
B = [B11 B12 B16; B12 B22 B26; B16 B26 B66]


        %To calculate D Matrix

        D11_test=Q11_bar(1,1)*(th*zkbar1^2 +(th^3/12)) + Q11_bar(1,2)*(th*zkbar2^2 +(th^3/12))+
Q11_bar(1,3)*(th*zkbar3^2 +(th^3/12)) +Q11_bar(1,4)*(th*zkbar4^2 +(th^3/12));

        D16_test=Q16_bar(1,1)*(th*zkbar1^2 +(th^3/12)) + Q16_bar(1,2)*(th*zkbar2^2 +(th^3/12))+
Q16_bar(1,3)*(th*zkbar3^2 +(th^3/12)) +Q16_bar(1,4)*(th*zkbar4^2 +(th^3/12));

        D22_test=Q22_bar(1,1)*(th*zkbar1^2 +(th^3/12)) + Q22_bar(1,2)*(th*zkbar2^2 +(th^3/12))+
Q22_bar(1,3)*(th*zkbar3^2 +(th^3/12)) +Q22_bar(1,4)*(th*zkbar4^2 +(th^3/12));

        D12_test=Q12_bar(1,1)*(th*zkbar1^2 +(th^3/12)) + Q12_bar(1,2)*(th*zkbar2^2 +(th^3/12))+
Q12_bar(1,3)*(th*zkbar3^2 +(th^3/12)) +Q12_bar(1,4)*(th*zkbar4^2 +(th^3/12));

        D26_test=Q26_bar(1,1)*(th*zkbar1^2 +(th^3/12)) + Q26_bar(1,2)*(th*zkbar2^2 +(th^3/12))+
Q26_bar(1,3)*(th*zkbar3^2 +(th^3/12)) +Q26_bar(1,4)*(th*zkbar4^2 +(th^3/12));

        D66_test=Q66_bar(1,1)*(th*zkbar1^2 +(th^3/12)) + Q66_bar(1,2)*(th*zkbar2^2 +(th^3/12))+
Q66_bar(1,3)*(th*zkbar3^2 +(th^3/12)) +Q66_bar(1,4)*(th*zkbar4^2 +(th^3/12));

D= [ D11_test D12_test D16_test; D12_test D22_test D26_test; D16_test D26_test D66_test]

%A,B,D Stiffness Matrix
H=[A B;B D];

%Display Results
S=[A11, D66_test,B16]
```